EM-Neuro Modeling Across Scales for Bioelectronic Medicine

Lecture 10: Non-Invasive Brain Stimulation & Temporal Interference

Esra Neufeld[*] and Taylor Newton[*†]

[*]IT'IS Foundation for Research on Information Technologies in Society

[†]Integrated Systems Laboratory, ETH Zurich

Course Outline

DATE	LECTURE THEME
19.02	Motivation, logistics & tooling (EN, TNE)
26.02	Ion channels & membranes (EN)
05.03	Axon models, activating functions & electrical stimulation (EN)
12.03	EM field simulation fundamentals & coupled EM-neuro workflows (EN)
19.03	Peripheral nerves & interfaces for bioelectronic medicine (EN)
26.03	Spinal cord stimulation for neuroprosthetics and pain management & low-frequency exposure safety (TNE)
02.04	Morphology, synapses, microcircuits; point vs spiking networks (TNE)
09.04	No class: Easter break
16.04	Neural mass & whole brain models; hybridization (TNE)
23.04	Recording modalities, signal content & the reciprocity theorem (TNE)
30.04	Non invasive brain stimulation & temporal interference (EN)
07.05	Image based/personalized treatment planning and optimization (TNE)
14.05	No class: Ascension Day
21.05	Verification, validation, UQ, and reproducibility (EN)
28.05	Project presentations & synthesis (EN, TNE)

Room: ETZ E7

13:15-14:00 Lecture

14:00-14:15 Break

14:15-15:00 Lecture

15:00-15:15 Break

15:15-16:00 Exercise

Recorded Lectures & Course Material

Provided Here

Exercise Outline

DATE	EXERCISE THEME
19.02	"Hello Neuron": integrate-and-fire in Python/NEURON
26.02	Point neuron phase portrait; basic time integration numerics
05.03	Recruitment prediction for myelinated axon using AF/GAF
12.03	EM (FEM) modeling of transcranial brain stimulation
19.03	Stimulation selectivity and signal content modeling for nerve interfaces
26.03	Mini project work
02.04	Mini project work
09.04	No class: Easter break
16.04	Guest (Neuromodulation Spin-Off – Z43)
23.04	Mini project work
30.04	Guest (NIBS – Kinderspital)
07.05	Guest (SCS – UNIL)
14.05	No class: Ascension Day
21.05	Mini project work
28.05	Project presentations

Room: ETZ E7

13:15-14:00 Lecture

14:00-14:15 Break

14:15-15:00 Lecture

15:00-15:15 Break

15:15-16:00 Exercise

Learning Objectives

- Distinguish tDCS, tACS, and TMS by mechanism, frequency content, and intended neural readout.
- Recall the quasi-static Poisson formulation for tES and explain why the quasi-static approximation is justified for typical tES/TI carrier ranges.
- Apply the somatic-polarization rule to estimate sub-threshold cortical effects of tES at typical doses [1][3][4].
- Understand the TI envelope-modulation formula for two locally superposed kHz electric fields and identify where the demodulation hypothesis is empirically supported and where it is contested [21][22][23].
- Describe a typical treatment planning workflow — inputs, outputs, and optimization objectives [10][16][38][53].
- Understand when TIS beats conventional tDCS for deep targets, and when it does not.
- Identify which uncertainties (skull conductivity [51], anatomical variability, active demodulation mechanism) motivate W11's personalization machinery.

Recommended Reading

- Grossman et al., Cell 169:1029 (2017) — founding TI paper [21]
- Mirzakhalili et al., Cell Systems 11:557 (2020) — biophysical critique of TI [22]
- Esmaeilpour et al., Brain Stimulation 14:55 (2021) — cortical co-activation argument [23]
- Violante et al., Nat. Neurosci. 26:1994 (2023) — first human deep-target TI [27]
- Karimi et al., J. Neural Eng. 22:026061 (2025) — IT'IS personalized NIBS pipeline & TI Planning Tool [10]
- Cassarà et al., Bioelectromagnetics 46:e22542, e22536 (2025) — TI safety recommendations, Parts I & II [32, 31]
- Rossi et al., Clin. Neurophysiol. 132:269 (2021) — TMS safety guidelines [14]

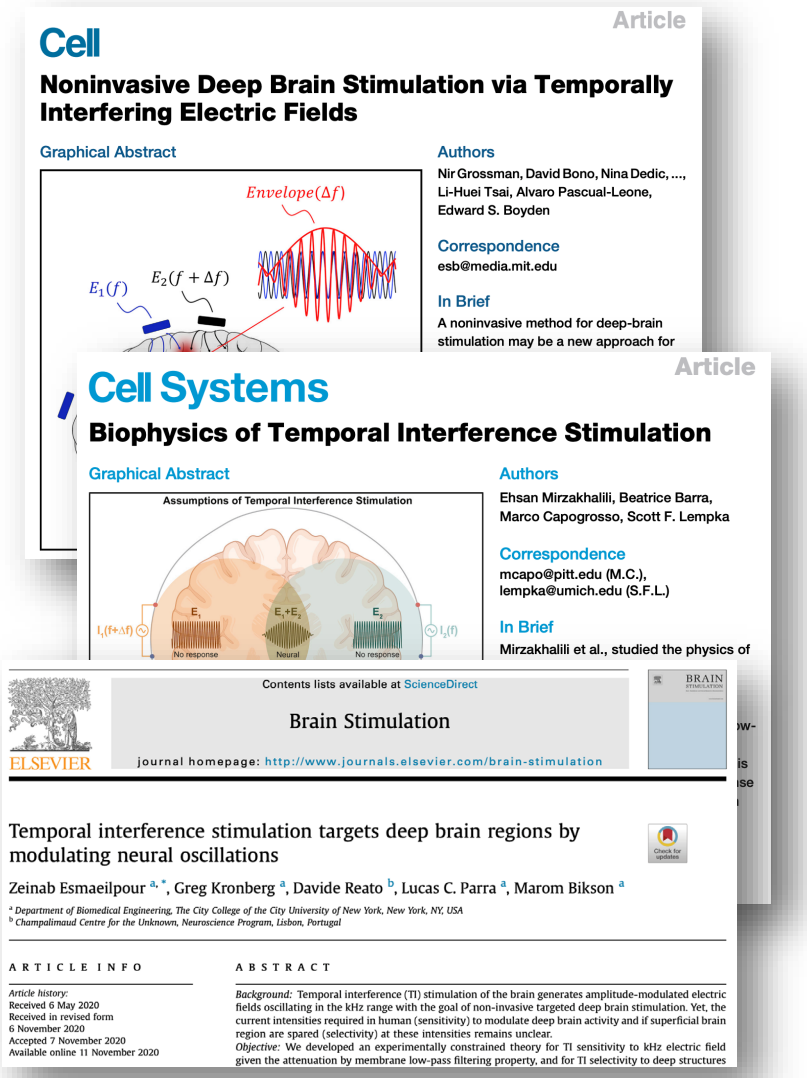

Outline for Today

- **Modalities at a glance — tDCS, tACS, TMS**
- Modeling tES forward fields — quasi-static, lead fields, somatic-polarization rule
- TMS field modeling and clinical translation — coil topographies, dosing, indications
- Temporal interference — the idea, the biophysics debate, recent human evidence
- Treatment planning & optimization — multi-objective targeting
- Exercise preview: Reto Huber (KISPI) — Non-invasive electric & acoustic brain stimulation

Non-Invasive Brain Stimulation

tDCS
transcranial direct current stimulation

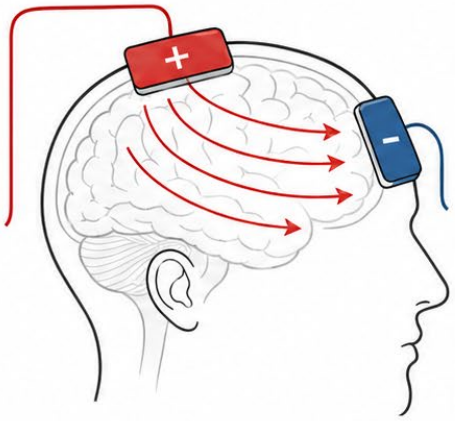

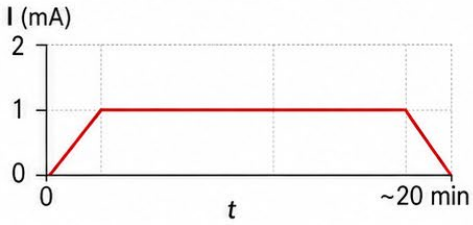

DC, 1–2 mA, ~minutes.

tACS
transcranial alternating current stimulation

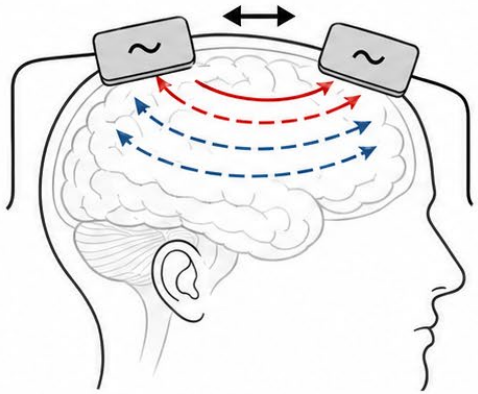

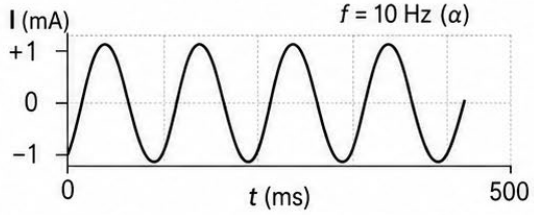

AC sinusoid, ~1–2 mA peak, target frequency (e.g., α: 10 Hz).

TMS
transcranial magnetic stimulation

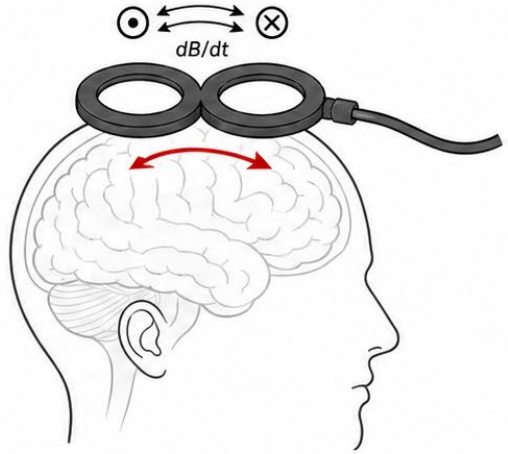

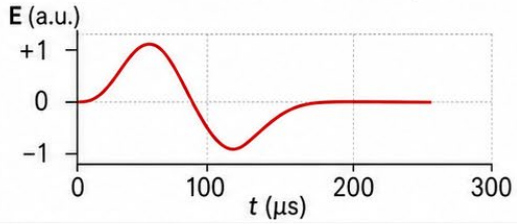

Pulsed, biphasic, ~100–300 µs; rTMS trains 1–20 Hz.

Different actuators, different time profiles — same underlying Maxwell physics.

Transcranial Direct Current Stimulation (tDCS)

- **What's delivered**: ~1–2 mA direct current (DC) scalp current, two or more pad/ring electrodes, 10–30 min sessions.
- **Intracerebral E-field**: a few tenths V/m per mA at typical cortical sites [3, 4]; intracranial peaks ~0.5 V/m / mA [5,6].
- **Mechanism**: sub-threshold somatic polarization of pyramidal neurons; anodal/cathodal rule is canonical for primary motor cortex (M1) [7], but polarity effects are orientation-, compartment-, folding-, montage-, and state-dependent.
- **Readout**: cortical-excitability shifts (motor evoked potential; MEP ±~30–40% for ~10 min after 9–13 min of 1 mA M1) [7].
- **Limits**: weak field, broad current paths, no focality without high-definition (HD) montages [3].

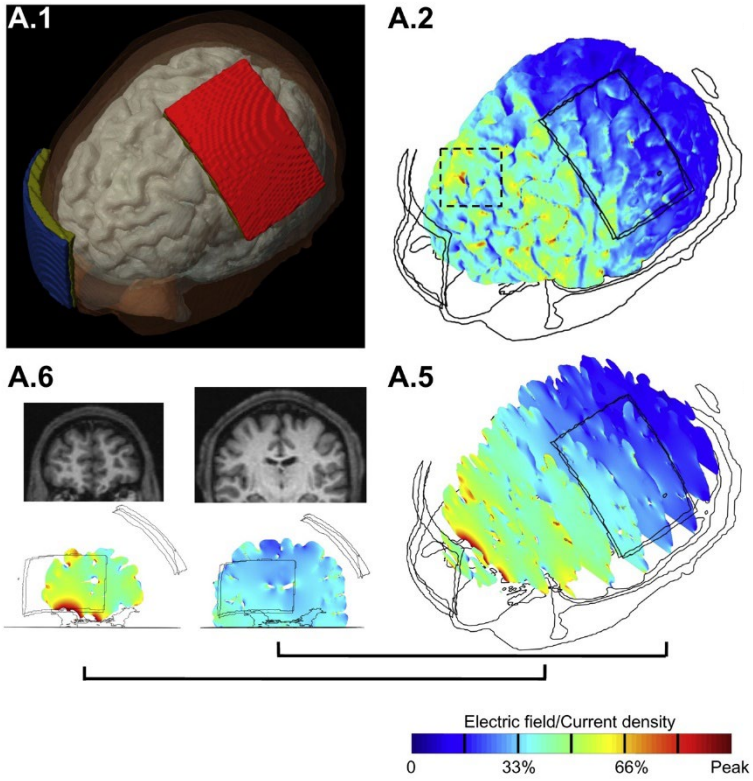

Brain modulation during transcranial direct current stimulation (tDCS) using conventional rectangular-pad configuration

Datta A et al., *Brain Stimulation*, 2009; 2, 201-207.e1

HD-tDCS: High-Definition Montages

HD 4×1 ring

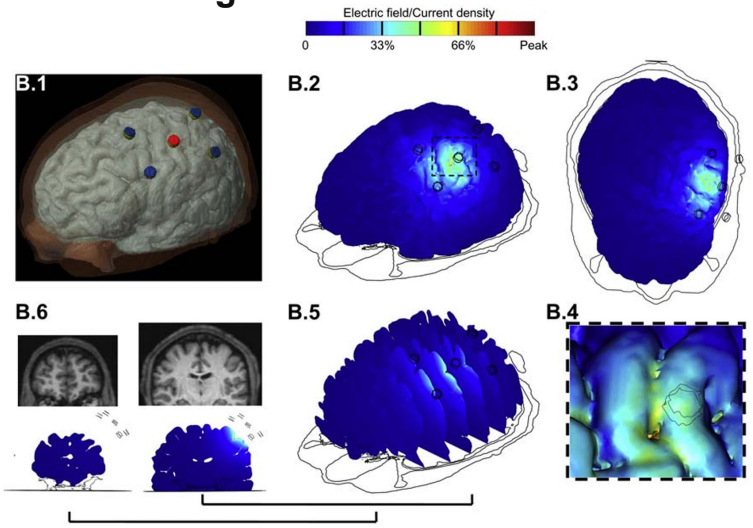

Datta A et al., *Brain Stimulation*, 2009; 2, 201-207.e1

Brain modulation during transcranial direct current stimulation (tDCS) using the 4x1 ring electrode configuration:
Local closure → sharper superficial focusing

- **Boundary-Condition Engineering:** HD-tDCS replaces large pads with distributed micro-electrodes to precisely shape scalp boundary conditions [3].
- **The 4x1 Ring:** The canonical montage uses one central active electrode (e.g., +2 mA) surrounded by four symmetric returns (e.g., -0.5 mA), satisfying charge conservation: $\sum I_k = 0$.
- **Physics of Confinement:** Geometry creates a localized source-sink structure, confining the current density field ($\mathbf{J} = \sigma\mathbf{E}$) and steepening the spatial gradient compared to diffuse standard pads.
- **The Depth-Focality Trade-off:** In quasi-static volume conduction (Laplace/Poisson), higher-spatial-frequency boundary patterns decay much faster with depth.

  $$\uparrow \text{focality} \Rightarrow \downarrow \text{depth reach}$$
- **Practical Consequence:** HD-tDCS is a superficial cortical shaping tool, not a deep-target solution.

Transcranial Alternating Current Stimulation (tACS)

- **Delivered**: sinusoidal scalp current, 1–2 mA peak, 0.1–130 Hz (mostly 4–40 Hz to match endogenous rhythms); pad electrodes.
- **Mechanism**: rhythmic sub-threshold polarization → state-supported phase-entrainment when stimulation frequency matches an existing / supported network rhythm [8][9].
- **Readout**: state-dependent enhancement/suppression of band-specific oscillations; e.g., 10 Hz parieto-occipital tACS modulates alpha and target detection phase-dependently [9].
- **Mechanistic refinement**: ferret + model evidence — entrainment via fast-spiking interneuron phase-locking at moderate fields [33].
- **Caveat**: transcutaneous retinal phosphenes at 5–40 Hz can confound blinding [34].

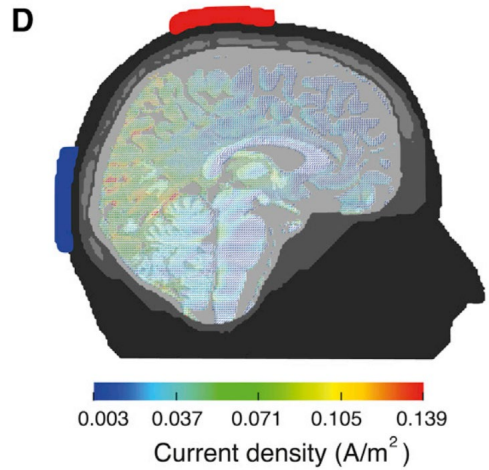

Helfrich RF et al., *Curr Biol.* 2014 Feb 3;24(3):333-9.

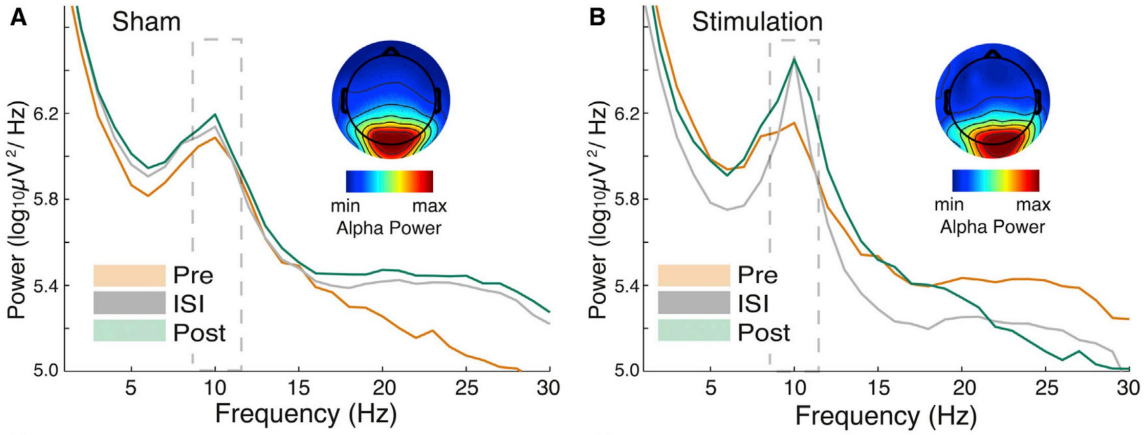

Transcranial Magnetic Stimulation (TMS)

- **Mechanism**: Coil drive I(t) → magnetic vector potential **A**(**r**,t), with **B** = ∇×**A**; by Faraday, induced primary field $\mathbf{E}_i = -\partial\mathbf{A}/\partial t$ scales with dI/dt.
- **Tissue formulation**: total $\mathbf{E} = -\nabla\varphi - \partial\mathbf{A}/\partial t$. $-\partial\mathbf{A}/\partial t$ term is the primary driver in TMS; $-\nabla\varphi$ captures charge accumulation at σ-boundaries. tES is recovered in the $\partial A/\partial t \to 0$ limit (preview of slide 14).
- **Delivered**: brief (~100–300 μs) pulsed B (peak ~1–2 T) → induced cortical E-field
- **Peak intracerebral E-field**: ~50–150 V/m (one to two orders above tES) → suprathreshold; coil/distance/pulse-shape-dependent.
- **Readout**: single pulse to M1 → contralateral MEP; repetitive TMS (rTMS; 1 Hz, 10 Hz, theta-burst) → lasting excitability changes.
- **Site of activation** (preview Part III): axons at bends, branch points, terminations — not somata [11, 12, 52].
- **Frequency content**: broadband; pulse-shape and stimulator-dependent.

Dufor, T et al., *Int. J. Mol. Sci.* **2023**, *24*, 16456.

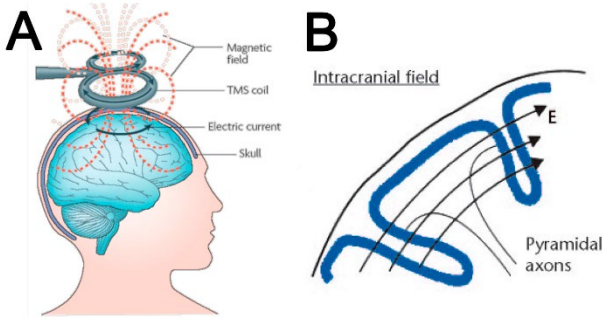

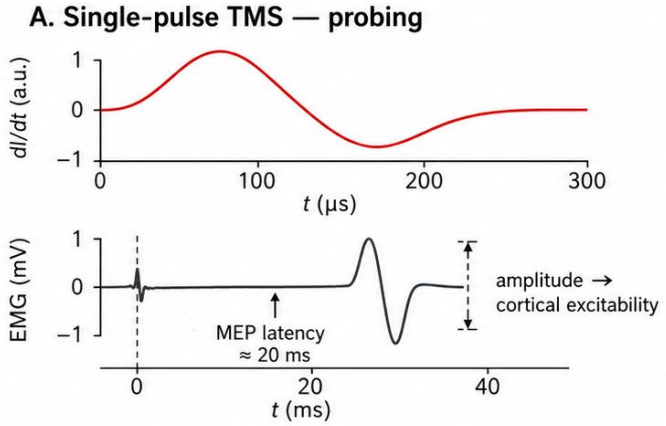

One pulse → one cortical event.
Used for: motor mapping, resting motor threshold (RMT), corticospinal excitability.

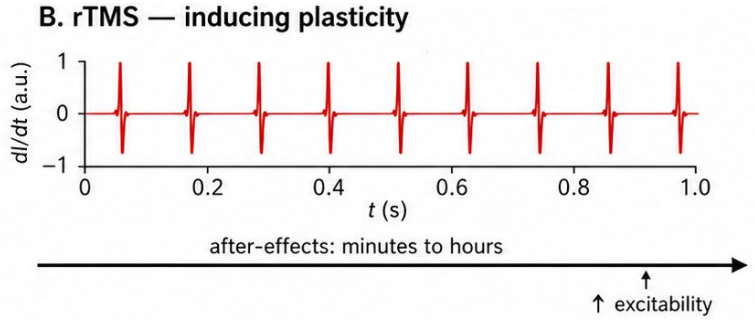

Trains of pulses → durable shifts in cortical excitability.
Used clinically: depression, OCD, stroke recovery.

Transcranial Magnetic Stimulation (TMS)

- **Mechanism**: Coil drive I(t) → magnetic vector potential **A**(**r**,t), with **B** = ∇×**A**; by Faraday, induced primary field $\mathbf{E}_i = -\partial\mathbf{A}/\partial t$ scales with dI/dt.
- **Tissue formulation**: total $\mathbf{E} = -\nabla\varphi - \partial\mathbf{A}/\partial t$. $-\partial\mathbf{A}/\partial t$ term is the primary driver in TMS; $-\nabla\varphi$ captures charge accumulation at σ-boundaries. tES is recovered in the $\partial A/\partial t \to 0$ limit (preview of slide 13).
- **Delivered**: brief (~100–300 µs) pulsed B (peak ~1–2 T) → induced cortical E-field
- **Peak intracerebral E-field**: ~50–150 V/m (one to two orders above tES) → suprathreshold; coil/distance/pulse-shape-dependent.
- **Readout**: single pulse to M1 → contralateral MEP; repetitive TMS (rTMS; 1 Hz, 10 Hz, theta-burst) → lasting excitability changes.
- **Site of activation** (preview Part III): axons at bends, branch points, terminations — not somata [11, 12, 52].
- **Frequency content**: broadband; pulse-shape and stimulator-dependent.

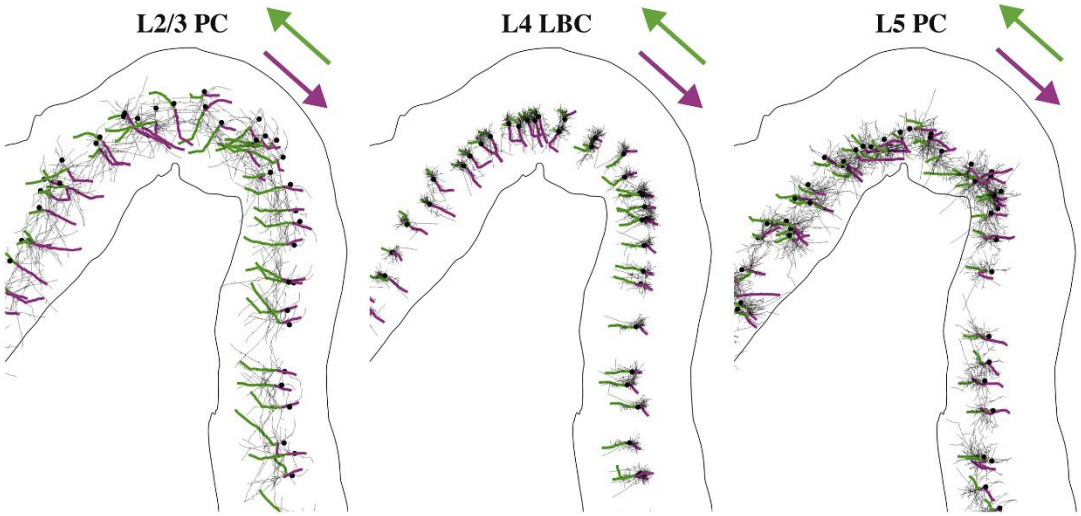

TMS activates axonal terminations aligned to local E-field direction. Axonal arbors for single population of L2/3 PCs, L4 LBCs, and L5 PCs with directly activated branch colored from AP initiation point (terminal) to proximal branch point for monophasic P–A (green) and A–P (magenta) stimulation.

Aberra A et al., *Brain Stimulation*, 2019; 13, 175-189

Comparing Across Modalities

**Values are order-of-magnitude.*

Modality	Driver	Scalp dose	Intracerebral E-field (typical/peak)	Frequency	Focality	Threshold
tDCS	DC current	1–2 mA	**~0.5 V/m at 1 mA [5]; ~0.8 V/m at 2 mA [6]**	0 Hz	low (cm)	sub-threshold
tACS	AC current	1–2 mA	**comparable to tDCS [5, 6]**	0.1–130 Hz	low	sub-threshold (entrainment)
TMS	Induced E (Faraday)	~1–2 T peak B	**~50–150 V/m**	broadband	~1–3 cm (figure-8)	supra-threshold
TI (preview)	Two kHz currents	2× ~2 mA (but up to 15 mA reported) [43]	**env. ~0.2–0.4 V/m, deep [27, 47]**	carrier 2-20 kHz [43] (unpublished: >80kHz), env. ~5–130 Hz	(claimed) deep & focal	sub-threshold

Outline for Today

- Modalities at a glance — tDCS, tACS, TMS
- **Modeling tES forward fields — quasi-static, lead fields, somatic-polarization rule**
- TMS field modeling and clinical translation — coil topographies, dosing, indications
- Temporal interference — the idea, the biophysics debate, recent human evidence
- Treatment planning & optimization — multi-objective targeting
- Exercise preview: Reto Huber (KISPI) — Non-invasive electric & acoustic brain stimulation

Refresher: Electro-Quasi-Static Poisson

- At <10 kHz in head tissue, inductive coupling and displacement currents are negligible vs. ohmic conduction.
- Forward problem → scalar quasi-static Poisson:

$$\nabla \cdot \left(\boldsymbol{\sigma}(\mathbf{r})\nabla\varphi(\mathbf{r})\right) = 0,$$
$$\mathbf{E} = -\nabla\varphi$$

  - σ anisotropic in white matter (DTI-derived tensor [10]); isotropic and weakly frequency-dependent elsewhere [35].
  - BCs: Dirichlet (constant potential) at electrodes—normalized later to unit current by integrating current flux density; insulating elsewhere. (Also: finite electrode potentials, contact impedance, and integral current constraints.) $(n \cdot \sigma\nabla\varphi = 0)$.
  - Caveat: dispersion (frequency-dependent σ, non-zero displacement currents) becomes non-negligible at 20–50 kHz carriers — see slide 27.
- Linearity: φ linear in injected currents → exact superposition. Foundation of basis-and-recombine optimization [10].

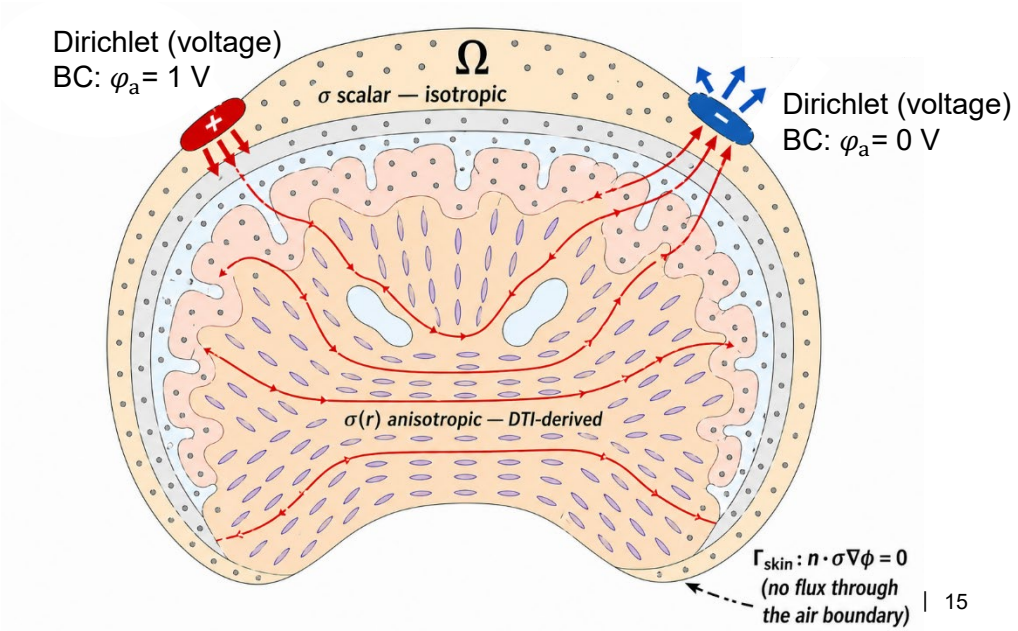

Refresher: Lead Field Operator

#simulations = #sources (~10k)
#simulations = #sensors (~100)

$$V_{ab} I_{ab} = -\mathbf{p}(\mathbf{r}) \cdot \mathbf{E}(\mathbf{r})$$

- From W09: recording lead field $\mathbf{V} = \mathbf{L} \cdot \mathbf{p}$ (sources $\mathbf{p}$ → scalp voltages).
- Reciprocal operator (W10): same operator gives EEG sensitivity of pair k to a source at r AND the field at r from unit current through pair k. Concretely:
  - at r for unit current through pair k; precomputed once per head model.
  - I_k = current through pair k; user-controlled.
- Caveat: reciprocity is bilinear, not a literal matrix transpose. EEG and tES system matrices are transposes only under matched discretization, bases, and inner products [10]. The useful equivalence: same $\mathbf{e_k}(\mathbf{r})$ solves stimulation forward AND gives EEG sensitivity of pair k.
- Consequence: For N electrodes, basis has N-1 degrees of freedom (all electrode pairs are overcomplete)→ combinatorial search is linear-algebraic [10].

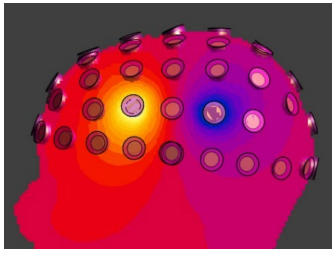

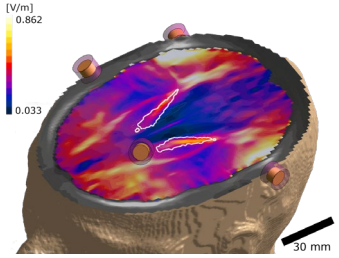

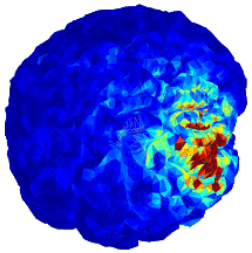

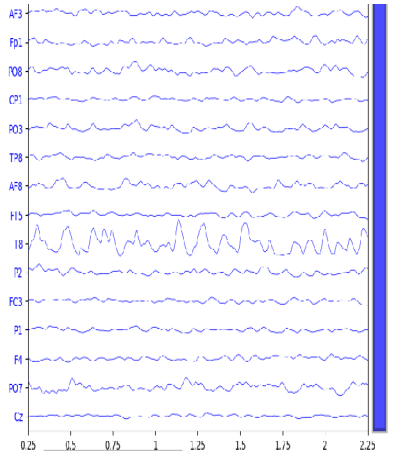

Quasi-Uniform Fields & Somatic Polarization

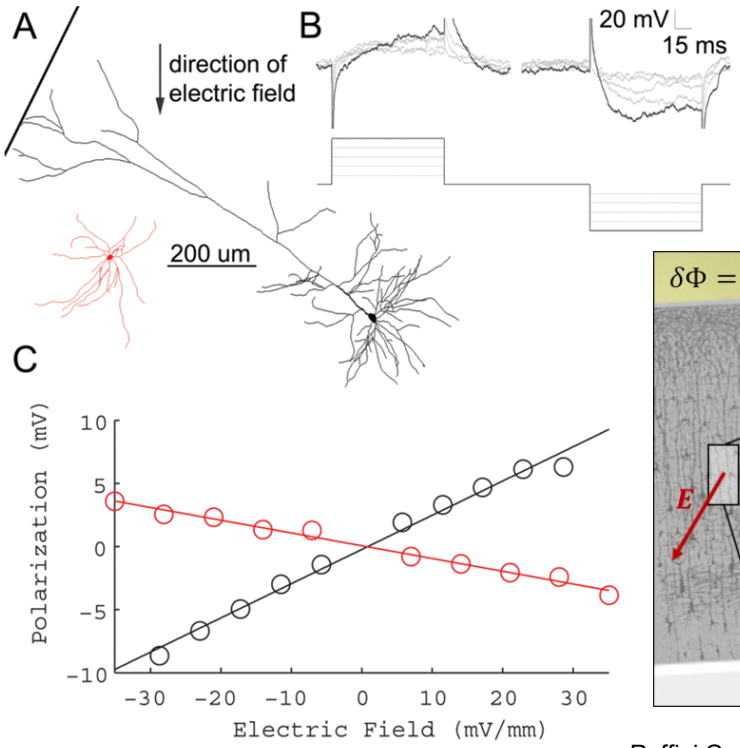

Radman T et al., *Brain Stimul.* 2009 Oct;2(4):215-28, 228.e1-3.

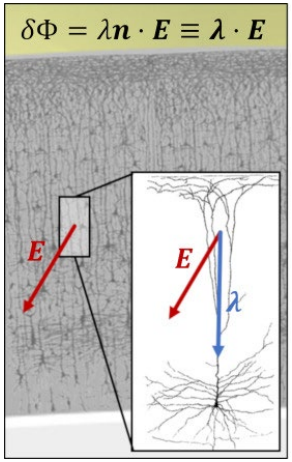

Ruffini G et al., *PLoS Comput Biol* 16(6): e1007923.

- Quasi-uniform field: tES E-field varies negligibly at neuron scale (~mm). Neuron sees uniform extracellular field [36].
- Somatic polarization rule (cortical pyramidal cells):
  - Somatic polarization linearly related to directionally align E-field via "λ" coupling term ($\lambda\hat{\mathbf{n}} \cdot \mathbf{E}$): **~0.2 mV per V/m**, along somato-dendritic axis (rat L5: 0.27; CA1: 0.12 mV/(V/m)) [1,2].
  - Pyramidal apical dendrite aligned with cortical normal → largest polarization per unit field; FS interneurons ~0.02 mV/(V/m) [1].
  - But network readout can be interneuron-mediated [33]; *per-neuron polarization ≠ which population dominates ≠ effective polarization in network (see next slide)*

- Typical tES dose: ~0.3 V/m × 0.2 mV/(V/m) ≈ **tens of µV** — far below ~15–25 mV spike threshold. tES is a bias, not a driver.
- Small persistent biases shift firing probability and entrain ongoing oscillations [7,9].

Quasi-Uniform Fields & Somatic Polarization

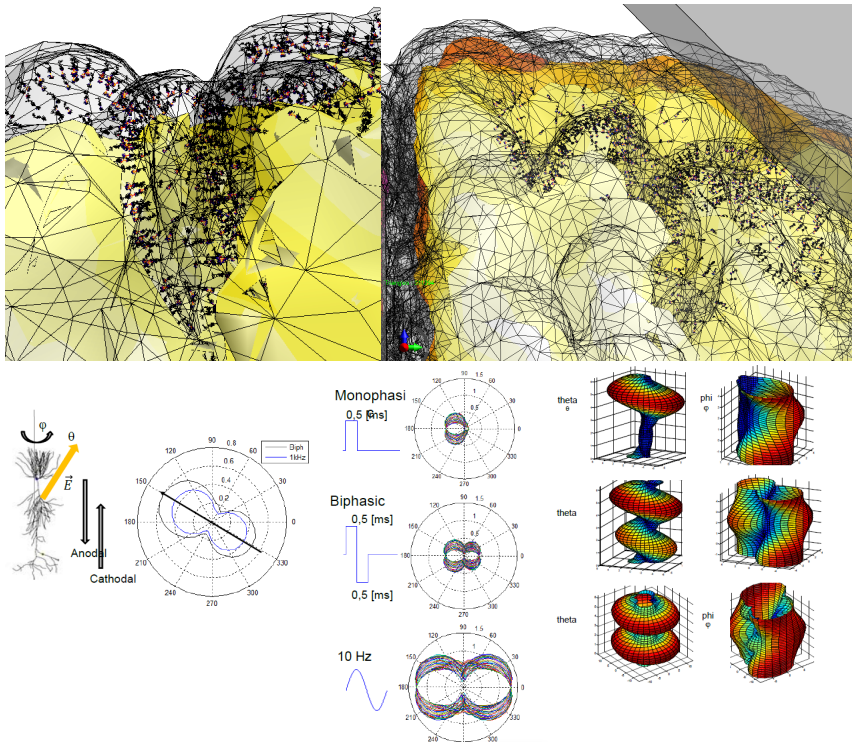

Cassarà, A.M., Neufeld, E., et al, N. Proceedings of the Joint Meeting of the Bioelectromagnetics Society (BEMS) and the European BioElectromagnetics Association (EBEA), Ghent, Belgium, 2016

- Quasi-uniform field: tES E-field varies negligibly at neuron scale (~mm). Neuron sees uniform extracellular field [36].
- Somatic polarization rule (cortical pyramidal cells):
  - Somatic polarization linearly related to directionally align E-field via "λ" coupling term ($\lambda\hat{\mathbf{n}} \cdot \mathbf{E}$): **~0.2 mV per V/m**, along somato-dendritic axis (rat L5: 0.27; CA1: 0.12 mV/(V/m)) [1,2].
  - Pyramidal apical dendrite aligned with cortical normal → largest polarization per unit field; FS interneurons ~0.02 mV/(V/m) [1].
  - But network readout can be interneuron-mediated [33]; *per-neuron polarization ≠ which population dominates ≠ effective polarization in network (see next slide)*

- Typical tES dose: ~0.3 V/m × 0.2 mV/(V/m) ≈ **tens of µV** — far below ~15–25 mV spike threshold. tES is a bias, not a driver.
- Small persistent biases shift firing probability and entrain ongoing oscillations [7,9].

Emerging Approaches to E-Field-Neuron Coupling

- Interactions between different cell types generate rhythms, synchrony, and collective oscillations
- Population-level patterns can amplify, cancel, or reshape how stimulation affects the network
- Neural mass models (NMMs) capture these emergent dynamics by representing an entire interacting population as a single unit (W08)

- New approaches investigate the interaction of weak E-fields and neural populations, not just single cells:
  - Find a semi-empirical meso-scale "λ"
  - Allows for better insight into the relationship between the applied field and population activity
  - Relevant for coupling NMMs to tES, TIS, TMS etc.

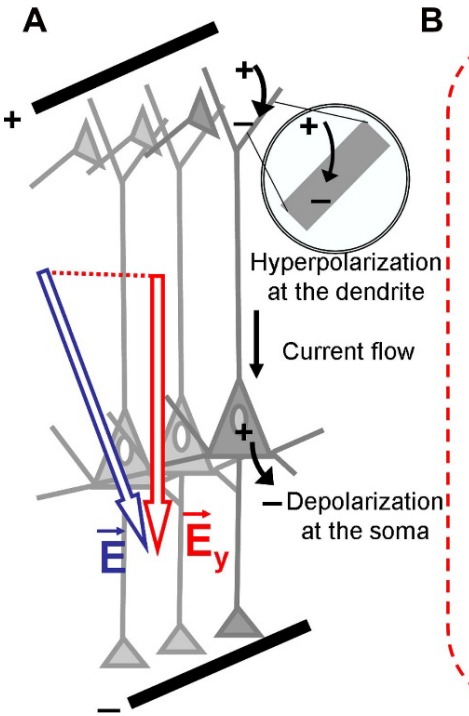

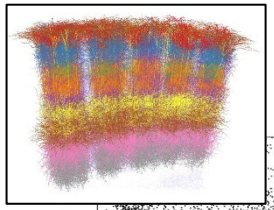

Molaee-Ardekani B et al., *Brain Stimul.* 2013 Jan;6(1):25-39.

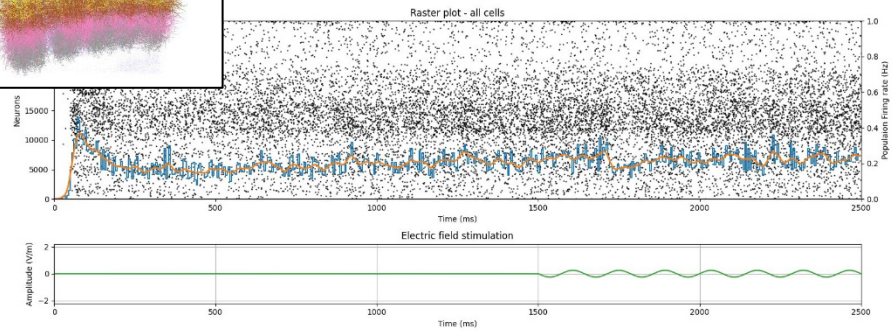

Variability, Uncertainty & Personalization (→ W11)

- Skull conductivity = dominant FEM uncertainty.
  - Reported σ_{skull} spans ~0.003–0.033 S/m (~10× range) [51].
  - Skull = largest series resistor; σ_{skull} uncertainty propagates ~linearly to intracerebral E-field.
- Other uncertainties: WM anisotropy (DTI tensors [10]), CSF segmentation errors, electrode–skin contact impedance, brain drift in cerebrospinal fluid (CSF), age/pathology effects.
- Inter-subject variability: ~2–3× in target E-field under fixed montages [29].
- Consequence: generic montages → generic outcomes. Personalization (W11) is key for reproducible dosing.

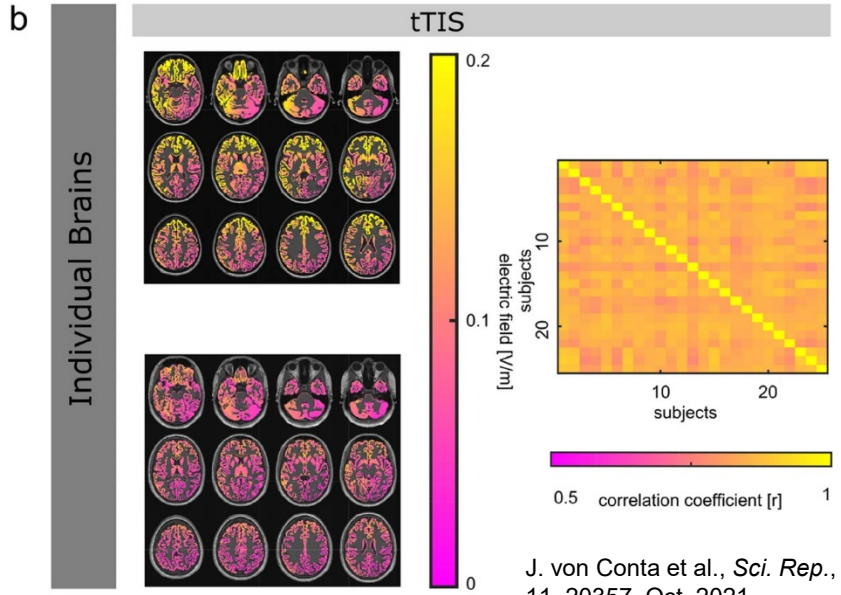

J. von Conta et al., *Sci. Rep.*, vol. 11, 20357, Oct. 2021.

Temporal Interference

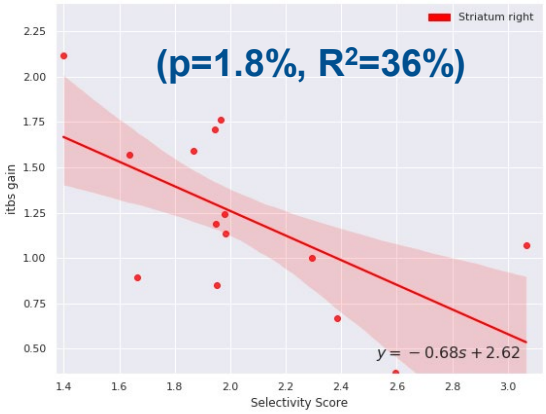

High-Frequency Control

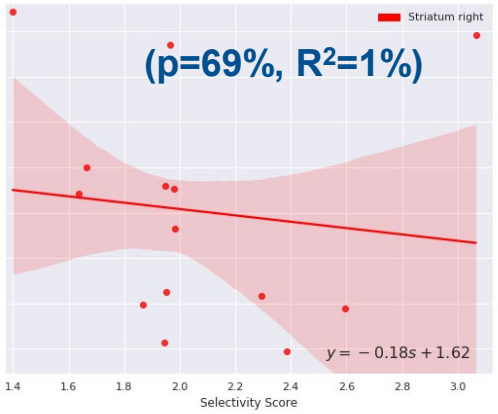

Outline for Today

- Modalities at a glance — tDCS, tACS, TMS
- Modeling tES forward fields — quasi-static, lead fields, somatic-polarization rule
- **TMS field modeling and clinical translation — coil topographies, dosing, indications**
- Temporal interference — the idea, the biophysics debate, recent human evidence
- Treatment planning & optimization — multi-objective targeting
- Exercise preview: Reto Huber (KISPI) — Non-invasive electric & acoustic brain stimulation

Coil Geometries and Induced E-Field Topography

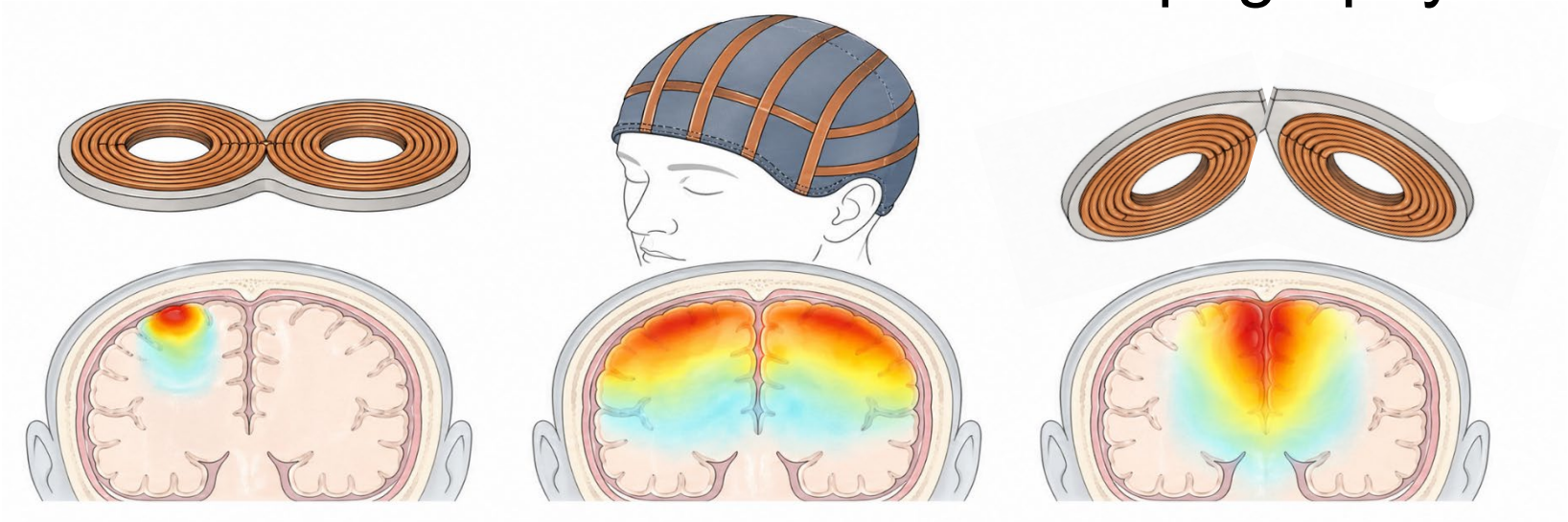

- **Figure-8 ("butterfly")** [17]: two co-planar windings, opposing currents; focal peak E at junction (~1–2 cm focality, ~1.5–2 cm depth). Standard for M1, dorso-lateral prefrontal cortex (DLPFC).
- **H-coil (Hesed)** [18, 19]: 3-D winding wrapping scalp; deeper penetration (~3–4 cm), poorer focality. Brainsway FDA-cleared for depression, smoking, OCD.
- **Double-cone** [20, 37]: two angled coils; deep midline reach (cingulate, leg M1), poorer focality.
- Trade-offs [37]: depth–focality is a physical constraint. Coils choose an operating point on the curve; specific values metric-dependent but the trade-off is robust.
- Modern targeting: subject-specific FEM (Sim4Life, SimNIBS) for field-informed dosing [16, 38].

Activating Function, Axonal Bending & Tissue σ Contrast

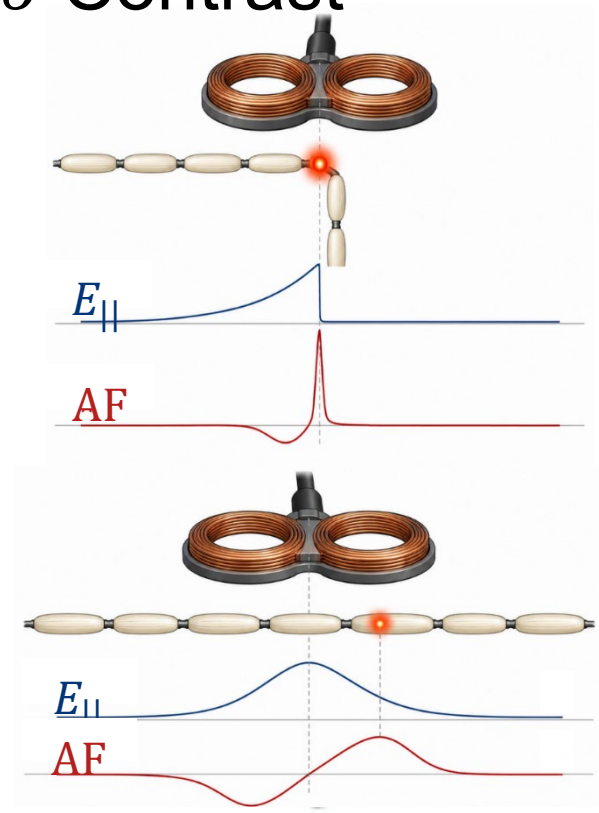

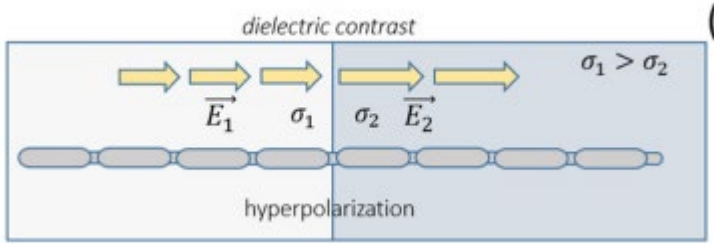

- Long straight axon in external E-field — driving term of the cable equation is the activating function (AF) [52]: $\mathrm{AF} \propto \frac{\partial^2 V_e}{\partial s^2} = -\frac{\partial E_{\|}}{\partial s}$
  - where s = arc length, V_e = extracellular potential, $\mathbf{E}_{\|} = \mathbf{E} \cdot \hat{\mathrm{s}}$ (E-field along axon)
  - Excitation where AF > 0 and exceeds threshold (n.b. sign conventions).
- TMS activates axons at bends/terminations/WM-GM interface [11, 12, 52]:
  - At a bend or termination, $\partial E_{\|}/\partial s$ can cause spike even when field is smooth.
  - Bends reduce threshold by >2× [12].
  - WM-GM σ contrast also causes high $\partial E_{\|}/\partial s$ where axons cross → spiking.
- Consequence: TMS activates axonal microgeometry — gyral lips, gray/white matter transitions, collateral terminations — not "the cortex under the coil." Coil-centroid placement ≠ biophysically faithful targeting.

Dosing: Motor Threshold vs. E-Field-Informed

- Classical motor-threshold (MT) dosing [13]:
  - Resting MT = lowest %-output evoking ≥50 μV MEP on ≥5/10 pulses.
  - Therapeutic dose = fixed multiplier of MT (e.g., 120% RMT for MDD [24]).
  - Pros: simple, biologically grounded, individualized. Con: MT at M1 ≠ E-field at treatment target (e.g., DLPFC).
- seizure screening.

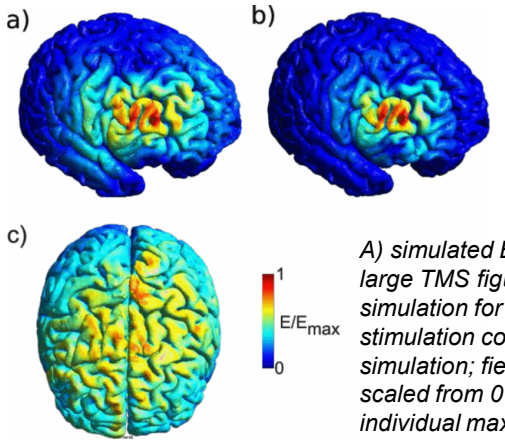

A) simulated E-field for a large TMS figure-8 coil. B) simulation for a focal stimulation coil. C) TDCS simulation; field strength scaled from 0 (blue) to the individual maximum (red).

A. Thielscher, et al., *2015 37th Annual International Conference of the IEEE Engineering in Medicine and Biology Society (EMBC)*, Milan, Italy, 2015

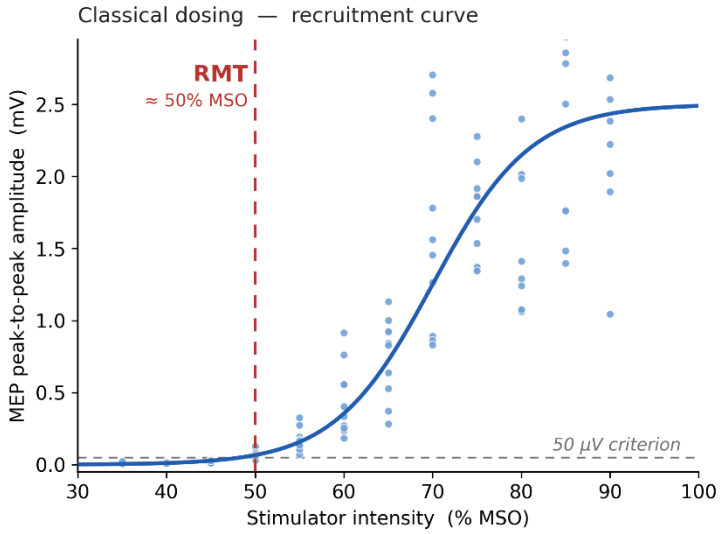

- E-field-informed dosing [16][38]:
  - Subject-specific FEM (Sim4Life/SimNIBS): MRI → mesh → coil placement → E at target.
  - Dose set to match target E-field (e.g., 100 V/m at DLPFC).
  - Pros: anatomically faithful, reduces dose variance. Cons: requires MRI + pipeline.

Repetitive TMS (rTMS) Clinical Translation

- Major depression (MDD):
  - NeuroStar figure-8, 10 Hz L-DLPFC, 120% RMT, 3000 pulses/day × 4–6 wk; pivotal RCT n=301 [24]; FDA 2008.
  - Multi-site observational study (n=307): 58% response, 37% remission [25].
  - SAINT/SNT: fMRI-guided intermittent theta-burst stimulation (iTBS); open-label SAINT reported ~90% remission [26]; double-blind RCT reported 79% remission in active SNT [26b]; FDA 2022 (Magnus).
- OCD: Brainsway at 20 Hz, pivotal RCT n=99 [39]; FDA 2018.
- Tobacco use: Brainsway H4 over insula/inferior PFC, 10 Hz; pivotal RCT n=262 [40]; FDA 2020 (first addiction clearance).
- Stroke motor recovery: NICHE RCT (n=199) — primary endpoint was **null result** (not different from sham) [41]. Field shifting to state-dependent, ipsilesional-excitatory, BCI-coupled, theta-burst protocols.
- Trend: "scalp landmark + motor threshold" → fMRI-targeted + E-informed dosing

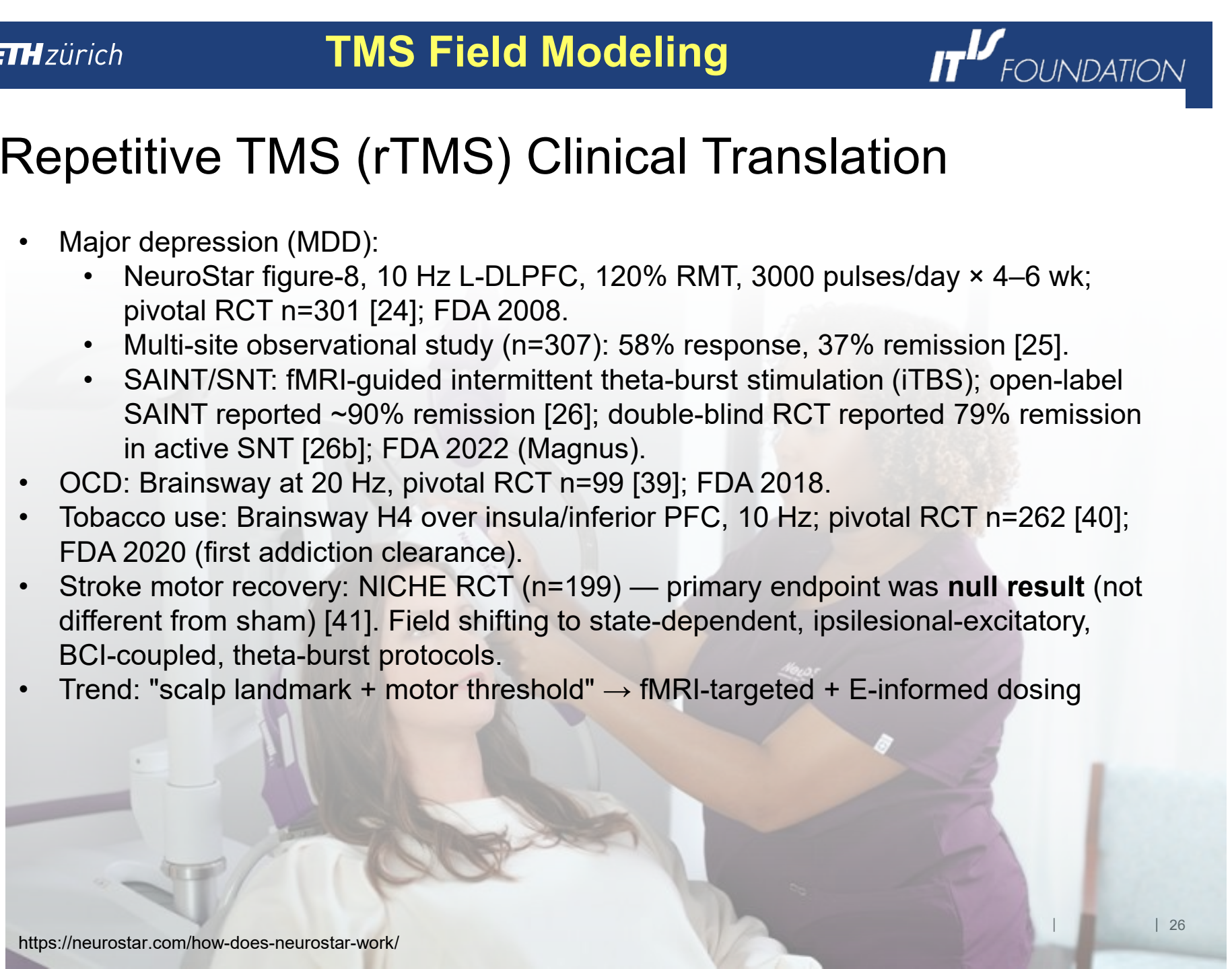

https://neurostar.com/how-does-neurostar-work/

Outline for Today

- Modalities at a glance — tDCS, tACS, TMS
- Modeling tES forward fields — quasi-static, lead fields, somatic-polarization rule
- TMS field modeling and clinical translation — coil topographies, dosing, indications
- **Temporal interference — the idea, the biophysics debate, recent human evidence**
- Treatment planning & optimization — multi-objective targeting
- Exercise preview: Reto Huber (KISPI) — Non-invasive electric & acoustic brain stimulation

The TI Envelope Equation

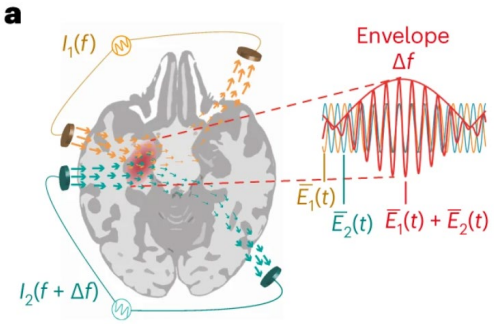

Violante, I.R., et al. *Nat Neurosci* 26, 1994–2004 (2023).

- Two kHz fields superimpose locally

$$\mathbf{E}(\mathbf{r}, t) = \mathbf{E}_1(\mathbf{r})\cos(2\pi f_1 t) + \mathbf{E}_2(\mathbf{r})\cos(2\pi f_2 t)$$
$$f_2 = f_1 + \Delta f, \quad \Delta f \ll f_1$$

- Assumption: neurons "see" the component along a sensitive direction $\hat{\mathbf{n}}$:

$$e_i(\mathbf{r}, \hat{\mathbf{n}}) = \mathbf{E}_i(\mathbf{r}) \cdot \hat{\mathbf{n}}$$

- Canonical Grossman case [21]: equal, collinear projected fields

$$e_1 = e_2 = E_0 \;\Rightarrow\; e(t) = 2E_0\cos(\pi\Delta f\, t) \cdot \cos\left[2\pi\left(f_1 + \frac{\Delta f}{2}\right)t\right]$$

→a kHz carrier whose amplitude is modulated at the beat frequency Δf.

- If projected magnitudes differ, TI becomes partial

$$A_{\max} = | e_1 | + | e_2 |,$$
$$A_{\min} = || e_1 | - | e_2 ||$$
$$E_{\mathrm{AM}} = A_{\max} - A_{\min} = 2\min(| e_1 |, | e_2 |)$$

for collinear projected fields

- **Interpretation:** the weaker projected field sets the modulation depth; the excess field remains as unmodulated kHz carrier.

Vector Nature of E & Neuron/Axon Orientation

- frequent misconceptions: don't expect fields to be aligned and proportional to currents
  - they don't compensate at 1:-1
  - the total field orientation is not constant
- sensitivity of neurons/axons/WM-tracts to exposure can be orientation dependent (e.g., polarizability)

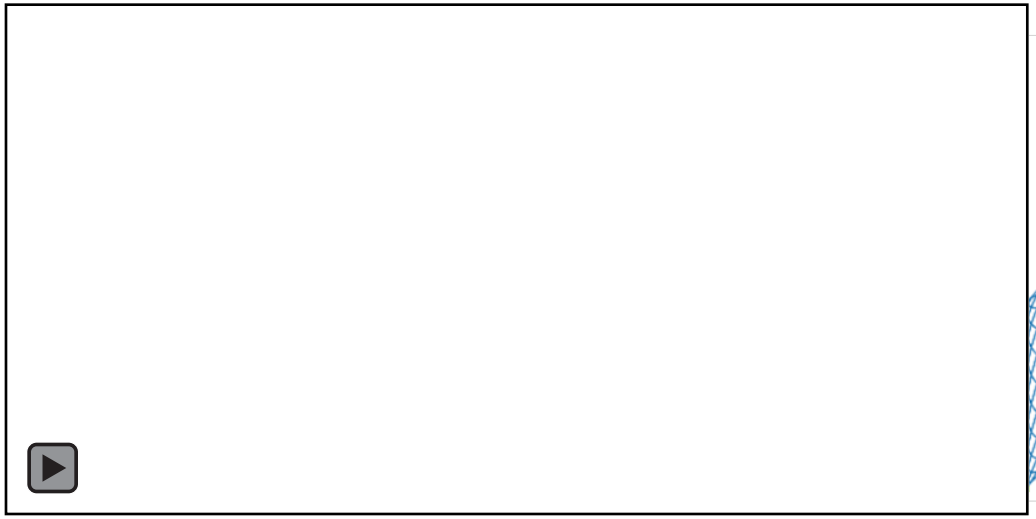

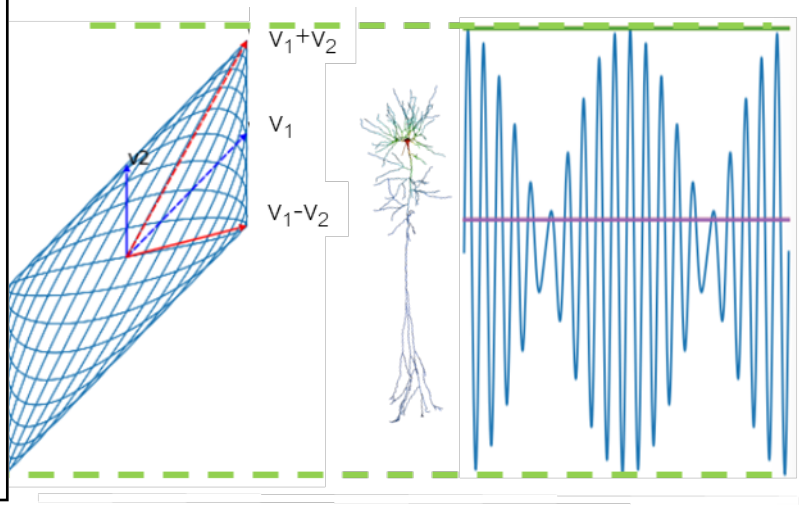

- frequent misconceptions: don't expect fields to be aligned and proportional to currents
  - they don't compensate at 1:-1
  - the total field orientation is not constant
- sensitivity of neurons/axons/WM-tracts to exposure can be orientation dependent (e.g., polarizability)

$$|TI(w_1,w_2)| = \begin{cases} 2\left|\overrightarrow{E_{2w}}(\vec{r})\right| \\ 2\left|\overrightarrow{E_{2w}}(\vec{r}) \times \left(\overrightarrow{E_{1w}}(\vec{r}) - \overrightarrow{E_{2w}}(\vec{r})\right)\right| / \left|\overrightarrow{E_{1w}}(\vec{r}) - \overrightarrow{E_{2w}}(\vec{r})\right| \end{cases} \text{ if } \begin{matrix} \left|\overrightarrow{E_{2w}}(\vec{r})\right| < \left|\overrightarrow{E_{1w}}(\vec{r})\right| \cos(\alpha) \\ otherwise \end{matrix} \quad [1]$$

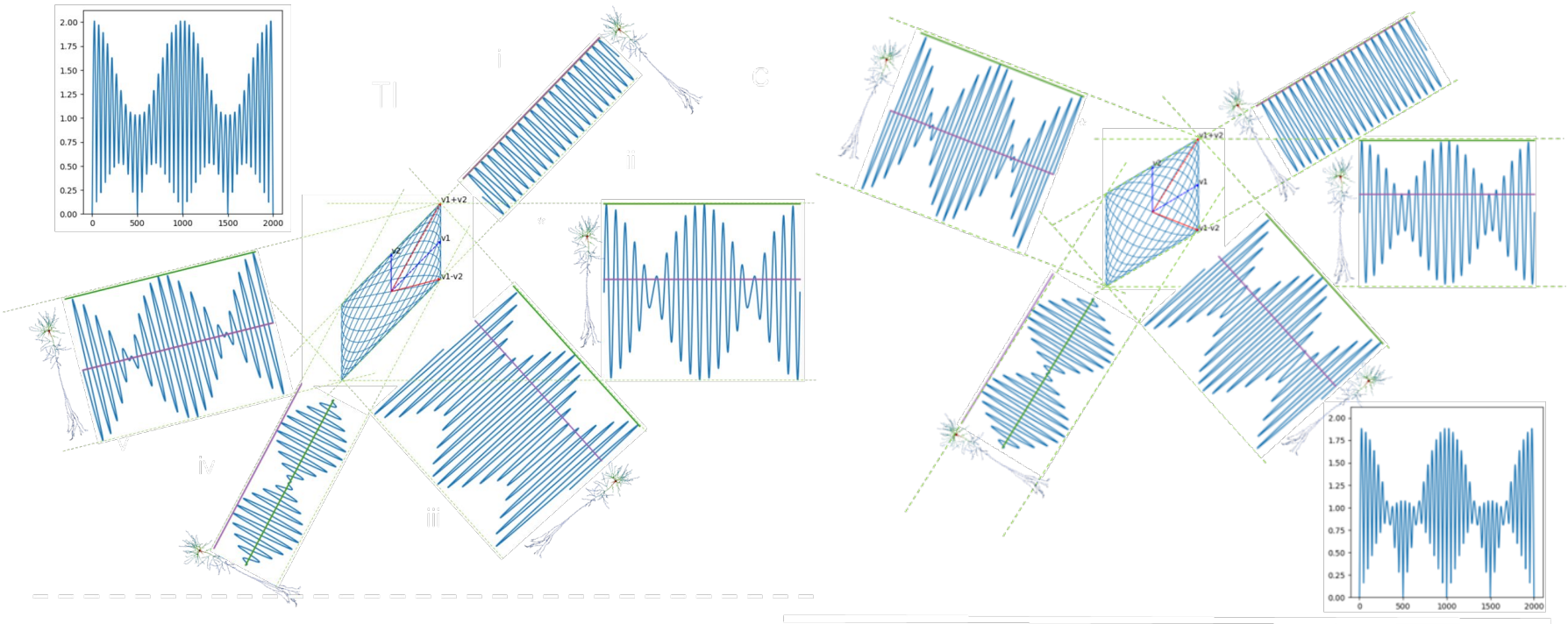

Vector Nature of E & Neuron/Axon Orientation

- frequent misconceptions: don't expect fields to be aligned and proportional to currents
  - they don't compensate at 1:-1
  - the total field orientation is not constant
- sensitivity of neurons/axons/WM-tracts to exposure can be orientation dependent (e.g., polarizability)

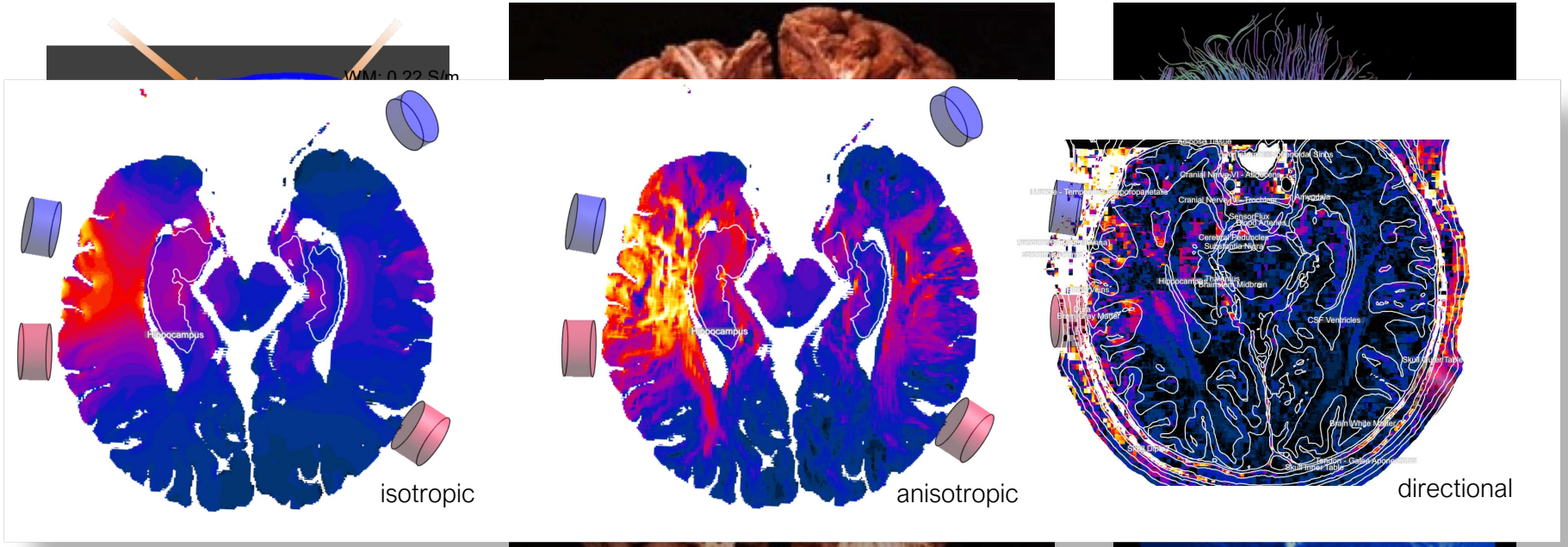

kHz: Safety and Effectivity

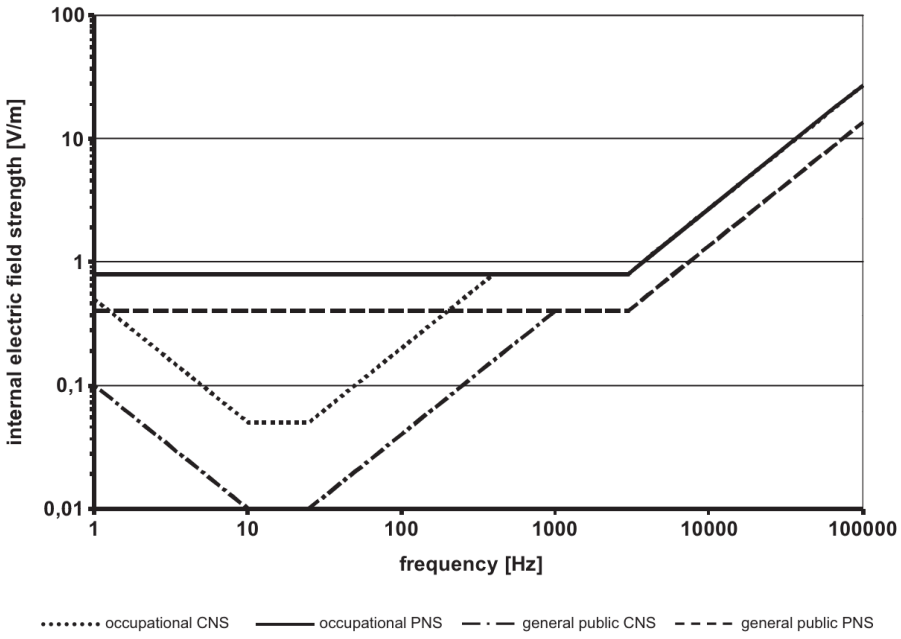

- **Principle**: ICNIRP basic restrictions on internal E-field rises with frequency above ~3 kHz [58] — kHz carriers have headroom that low-frequency tES does not.
- **Constraining limit is regime-dependent**: CNS/phosphene curve dips near 10–20 Hz (lowest allowed E); PNS curve flat to ~3 kHz, then ∝ f.
- **TI carriers exploit increasing limits**: 1–2 kHz on the plateau; >3 kHz on the rising CNS branch → larger allowed currents.

Note: limits are *internal* E-field (V/m in tissue), not injected current — translation requires a forward model.

kHz: Safety and Effectivity – TI [31,32]

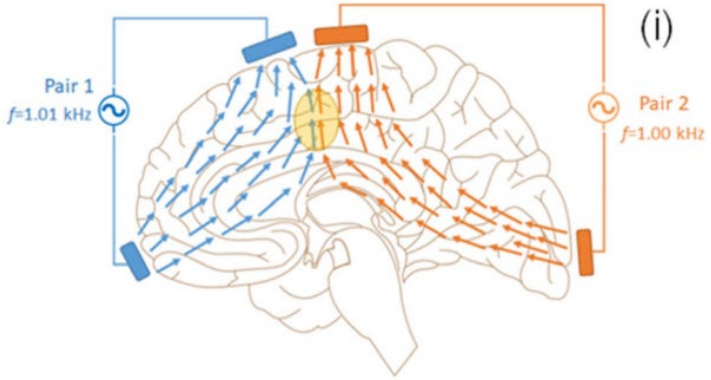

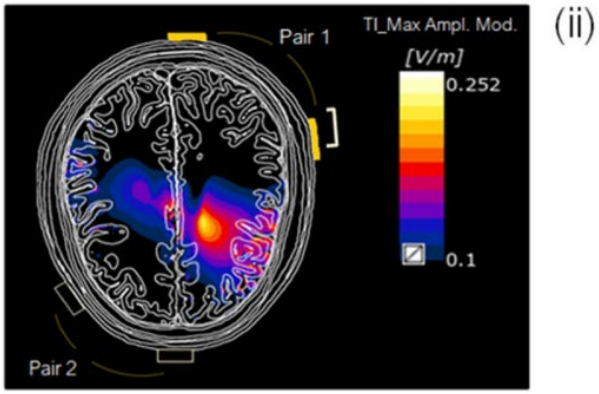

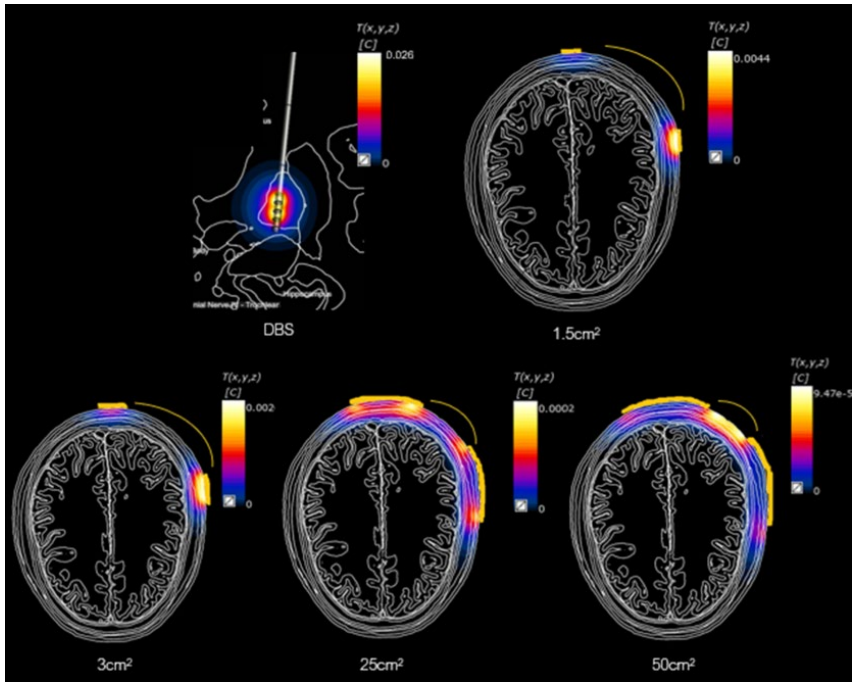

TABLE 3 | Proposed safety thresholds for TIS by exposure metric (3 cm^2 electrodes). Selection of exposure mechanisms was motivated by reported AEs. Thresholds are based on mechanistic considerations, dosimetric simulations of tDCS, tACS, DBS, and TIS, and the literature-informed history of safely applied conventional electrical stimulation. Thresholds are formulated in terms of measurable TIS application parameters (applied currents and voltages).

Metric	Relevance	< 2.5 kHz	2.5–100 kHz
E-field brain (peak)	Brain stimulation	16 mA (30 V/m, DBS outside stimulation zone)	16 mA × *f*/2.5 kHz (30 V/m × *f*/2.5 kHz, DBS outside stimulation zone)
E-field skin (peak)	Skin stimulation	**7 mA (200 V/m, tACS)**	**7 mA × *f*/2.5 kHz (200 V/m × *f*/2.5 kHz, tACS)**
Total current (peak)	Electrode–tissue interface effects	18 mA (DBS)	18 mA × *f*/2.5 kHz (DBS with frequency scaling)
Charge/phase (peak)	Electrochemistry	400 mA × *f*/1 kHz (1.3 mC, tACS)	400 mA × *f*/1 kHz (1.3 mC, tACS)
Brain temperature increase (peak)	Brain heating	14 mA (0.1°C, FDA)	**14 mA (0.1°C, FDA)**
Skin temperature increase (peak)	Skin heating	100 mA (2°C, FDA)	100 mA (2°C, FDA)
Applied voltage (peak-to-peak)	Leakage current	60 V (IEC/ISO 60601-1)	60 V (IEC/ISO 60601-1)

Note: Exposure quantities are shown in parentheses together with the reference application/standard used to define the threshold. All quantities are expressed as peak values (not RMS) except for applied voltage, which is formulated as peak-to-peak to ensure consistency with leakage current. Values in bold highlight the lowest effect thresholds and the metrics that may limit TIS exposure. All quantities were computed based solely on the direct effects of applied currents and voltages. IEC/ISO: joint technical committee of the International Organization for Standardization and the International Electrotechnical Commission. Stimulation zone: A sphere of radius 15 mm, centered on the DBS contacts (based on Medtronic 3389 neurostimulator) and encompassing the GP and the STN, beyond which stimulation effects are considered undesirable.

The TI Envelope Equation: Steering

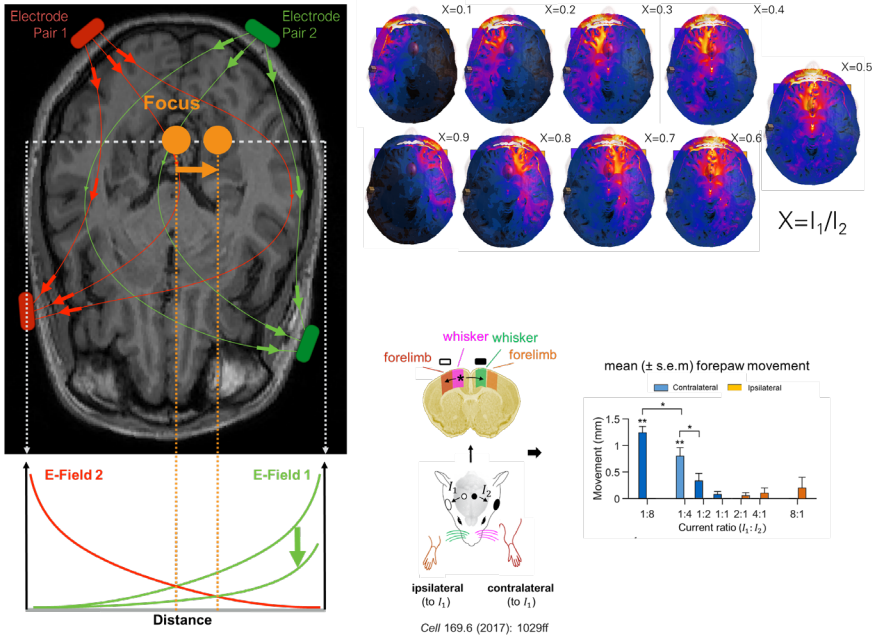

Images partially adapted from: Grossman N et al., Cell, 169, 1029-1041.e16

- **Targeting / steering:** electrode geometry and current ratios move the region where the two projected fields are large, roughly aligned, and sufficiently balanced. In [21], changing current ratios steered the motor response; hippocampal TI produced focal c-Fos at $f_1 \approx 2\,\mathrm{kHz}$, $\Delta f = 10\,\mathrm{Hz}$.

- **Phenomenological observation**: focus moves towards weaker current
- Consistent with modulation envelope magnitude being stimulation relevant QoI
- But the exact mechanism of TI is not yet understood

Biophysical Mechanisms: Membrane Demodulation?

- Proposed mechanism [21]: passive membrane low-pass reje
env
- τ_m
[42
cut
- Ob
ger
line
atte
is c

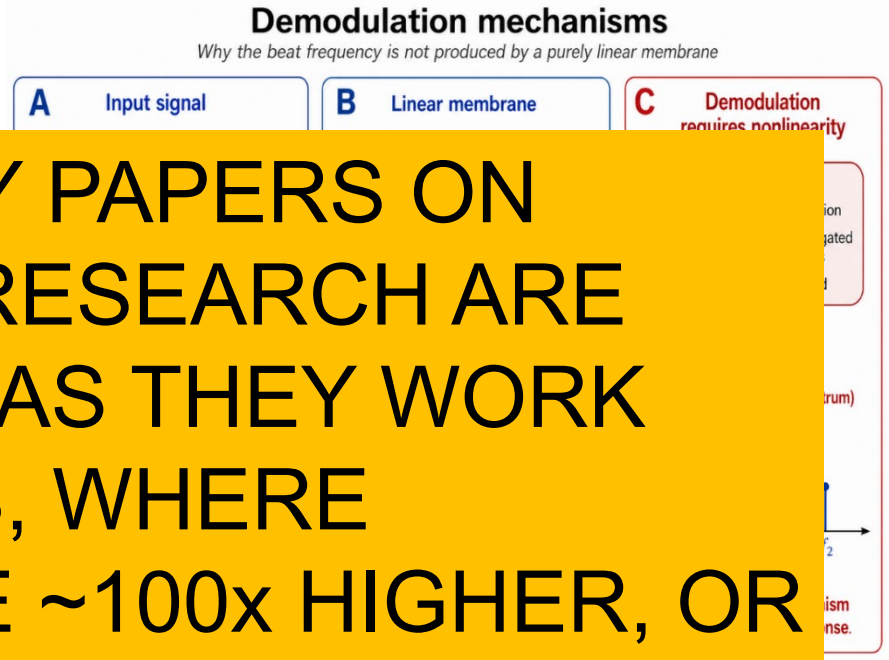

CAUTION: MANY PAPERS ON MECHANISTIC RESEARCH ARE PROBLEMATIC, AS THEY WORK WITH RODENTS, WHERE CURRENTS ARE ~100x HIGHER, OR THEY USE SUCH SUPRATHRESHOLD FIELD MAGNITUDES IN MODELING!!!

- Der
Na
driv
- Imp
den
needed.
- (different hypotheses for non-linearities not captured by HH-type models have been brought up, e.g., voltage depend. capacitance or conductance, periaxonal currents...)

Biophysical Mechanisms: Membrane Demodulation?

- Proposed mechanism [21]: passive membrane low-pass rejects kHz carriers, follows Δf envelope.
- τ_m ≈ 10–30 ms → f_c ≈ 5–15 Hz [42]. 2 kHz carrier ~200× above cutoff; 10 Hz envelope at cutoff.
- Objection [22]: linear filter cannot generate Δf — input has spectral lines only at f_1, f_2. Low-pass attenuates both; no Δf component is created.

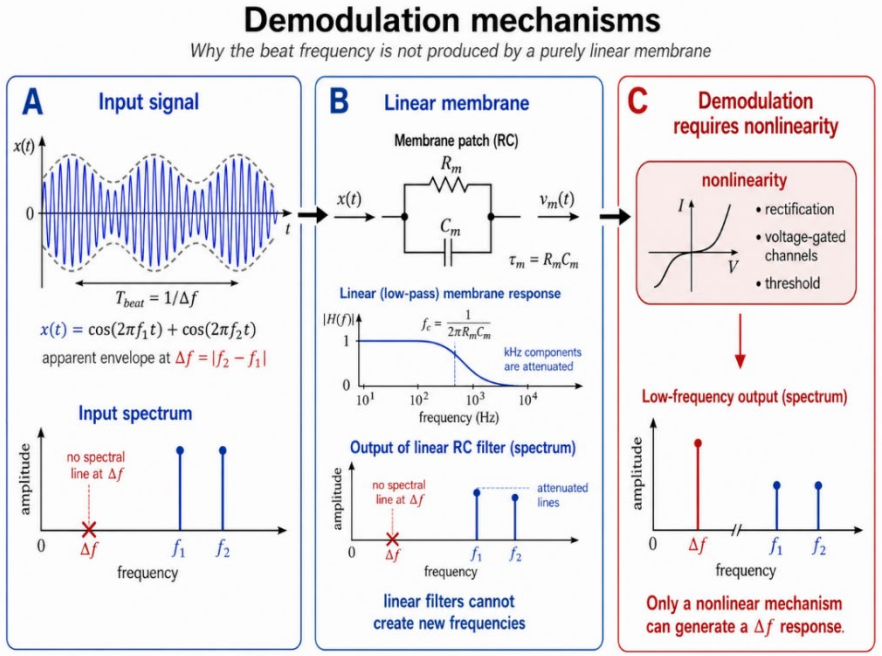

- Demodulation requires nonlinearity [22]: active ion-channel rectification (asymmetric Na^+/K^+ kinetics), engaged only at suprathreshold carriers — when the carrier itself drives spikes.
- Implication: at sub-threshold human fields (~0.3 V/m envelope [27]), passive demodulation does not straightforwardly apply. Subtler sub-threshold mechanisms needed.
- (different hypotheses for non-linearities not captured by HH-type models have been brought up, e.g., voltage depend. capacitance or conductance, periaxonal currents...)

The Cortical Coactivation Argument [23]

- Deep amplitude modulation (AM) can be steered — but superficial cortex sees large unmodulated carrier fields.
- Example model at 167 mA (n.b. too high for human use) [23]:
  - cortex near electrodes: unmodulated carrier $\approx$ $80\ \mathrm{V/m} \Rightarrow\approx 0.48\ \mathrm{V/m/mA}$
  - deep AM field: envelope $\approx$ $60\ \mathrm{V/m} \Rightarrow\approx 0.36\ \mathrm{V/m/mA}$

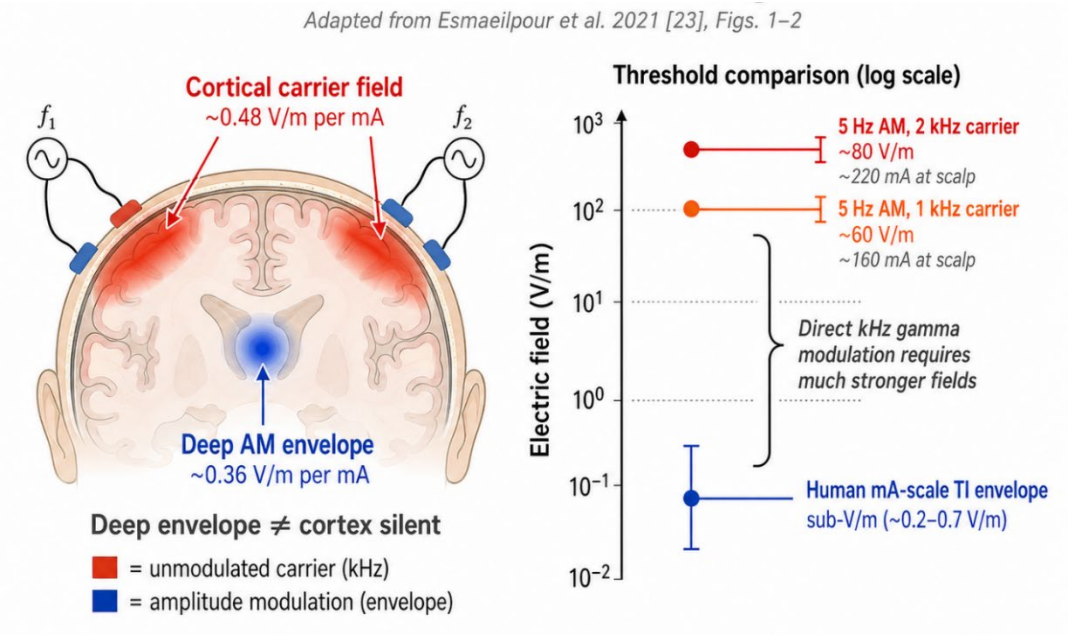

- **Proposed mechanism [23]**
  - Selectivity is *not* because cortex passively ignores the carrier.
  - Esmaeilpour's model proposes **network adaptation**, implemented as GABAB-mediated inhibition:
    - unmodulated kHz carrier → mainly static gamma-power modulation
    - AM kHz waveform → dynamic modulation at the beat frequency
  - Removing GABAB in the model reduced dynamic AM modulation and increased static response to unmodulated kHz.

TI Reaches Depth: Cadaver SEEG Validation [55]

Acerbo E et al., *Front. Neurosci.* 16:945221.

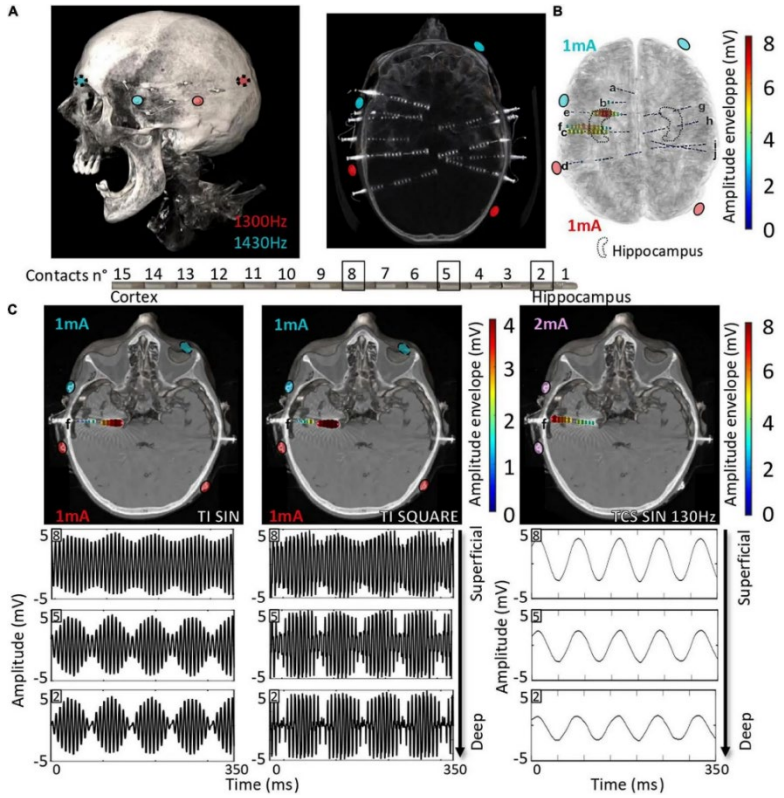

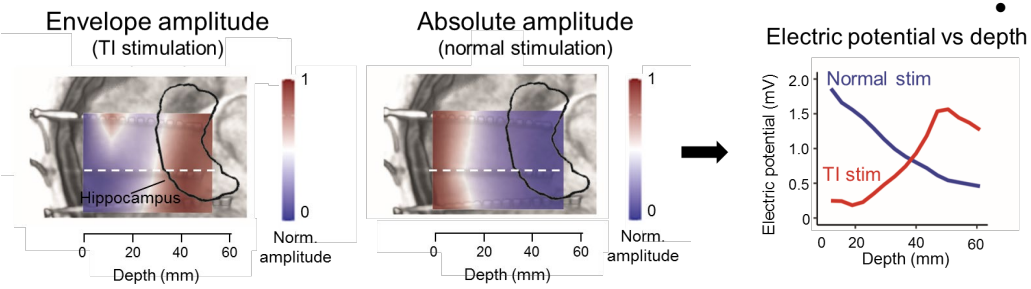

- **Setup**: 130 Hz TI envelope (1.30/1.43 kHz carriers) vs. 130 Hz transcranial current stimulation (TCS) via scalp; 12 SEEG leads, mainly temporal lobe, recorded intracranial fields in 2 perfused human cadavers [55].
- **Direct measurement at depth**: TI envelope extracted from SEEG recordings (not just simulated).
- **TI reaches depth**: ~7–8 mV envelope at hippocampal contacts; contralateral / non-hippocampal contacts ≈ 0 → focal hippocampal maximum.
- **TI vs. TCS**: along one SEEG track, TI envelope increased ~4× from superficial to deep contacts; 130 Hz TCS was largest near cortex and decayed with depth.
- **Waveform robustness**: Pulse width modulated (PWM)-TI (square waves) and sinusoidal TI produced similar depth profiles; PWM-TI used two offset square wave carriers.

Carrier Frequency Selection Trade-Offs

- **Field pattern:** for fixed montage/current and $f_c \lesssim 10\,\mathrm{kHz}$, E_{AM} is mainly set by geometry & current ratios.
- **Avoid carrier-only effects:** low-kHz carriers can suppress superficial cortical biomarkers; 9 kHz sham largely eliminated this effect in Missey/Acerbo et al. [44].
- **Target AM effect:** linear membrane intuition predicts weaker response at higher f_c:

$$|H_m(f_c)| \approx \frac{1}{\sqrt{1+(2\pi f_c \tau_m)^2}} \quad (-20\,\mathrm{dB/decade})$$

  but [44] found no detectable loss of 130 Hz hippocampal AM-TI suppression at 9 kHz vs. low-kHz carriers.

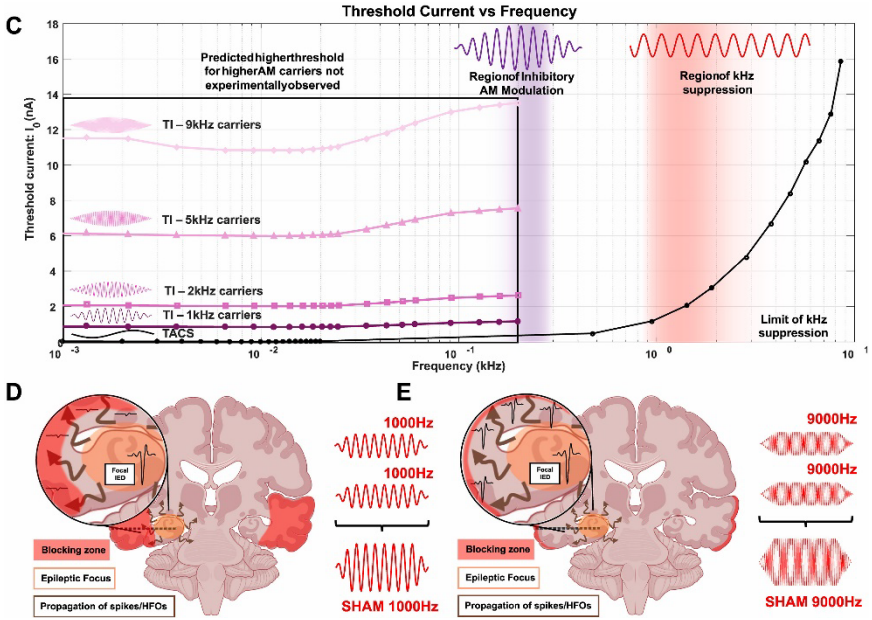

Esmaeilpour Z et al., *Brain Stimulation*, 2020; 14, 55-65

- **Tolerability / safety:** higher f_c may reduce scalp sensation, but high-f_c or high-current protocols must still check current density, heating, electrode interface, tissue dispersion, and stimulator bandwidth.
- **Current state:** ~2 kHz is historical convention, not an optimized choice. 9–20 kHz carriers are now being explored [43, 44].
- **Take-home:** choose f_c to reduce carrier-only off-target effects while preserving AM target effects; choose $\Delta f = |f_2 - f_1|$ for the target physiology.

Carrier Frequency Selection Trade-Offs

- **Field pattern:** for fixed montage/current and $f_c \lesssim 10\,\mathrm{kHz}$, E_{AM} is mainly set by geometry
- **A**
- **T**
- **T**
- **C**
- **Take-home:** choose f_c to reduce carrier-only off-target effects while preserving AM target effects; choose $\Delta f = | f_2 - f_1 |$ for the target physiology.

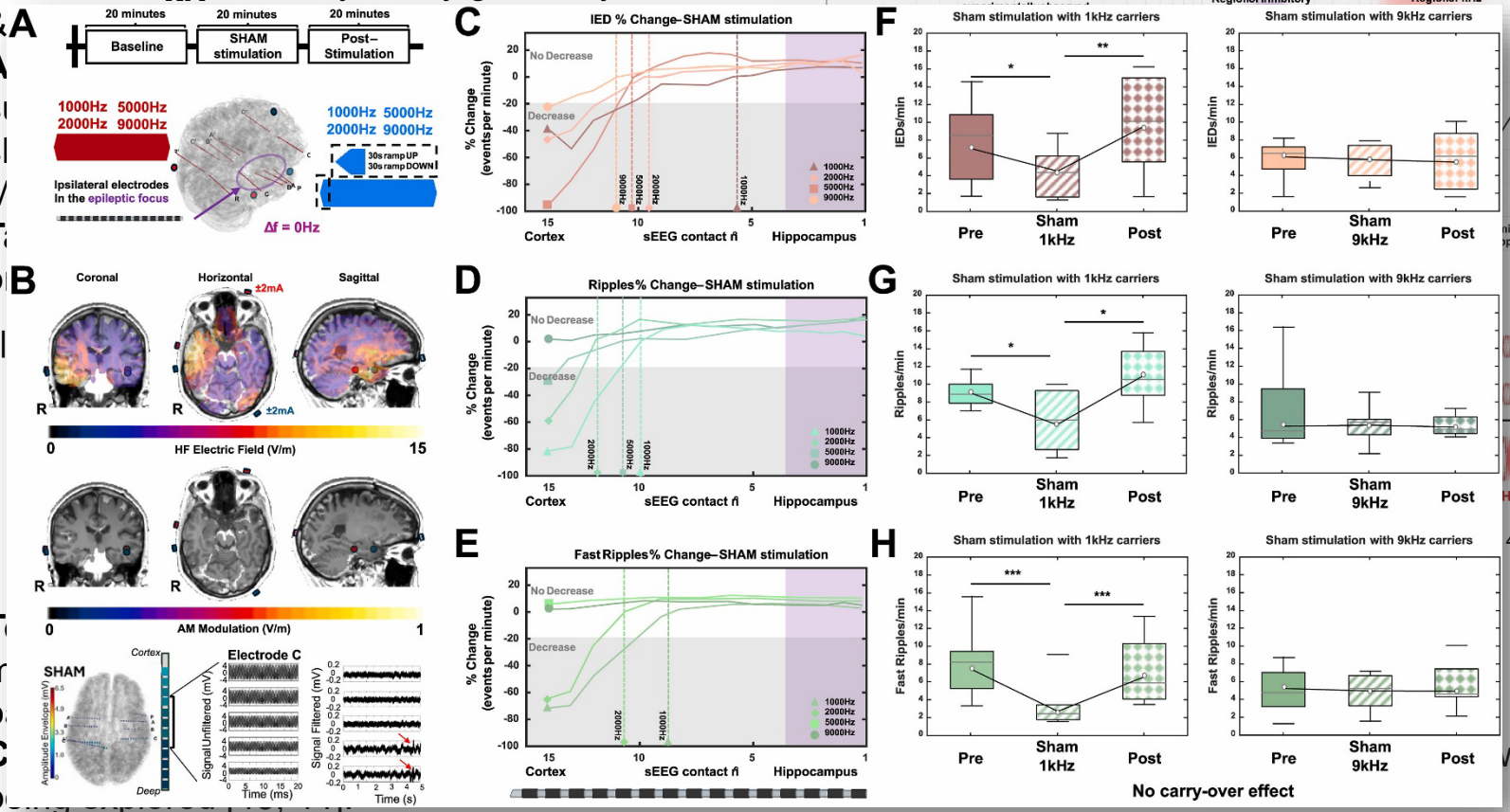

Suprathreshold Onset and Conduction-Block "Sandwich"

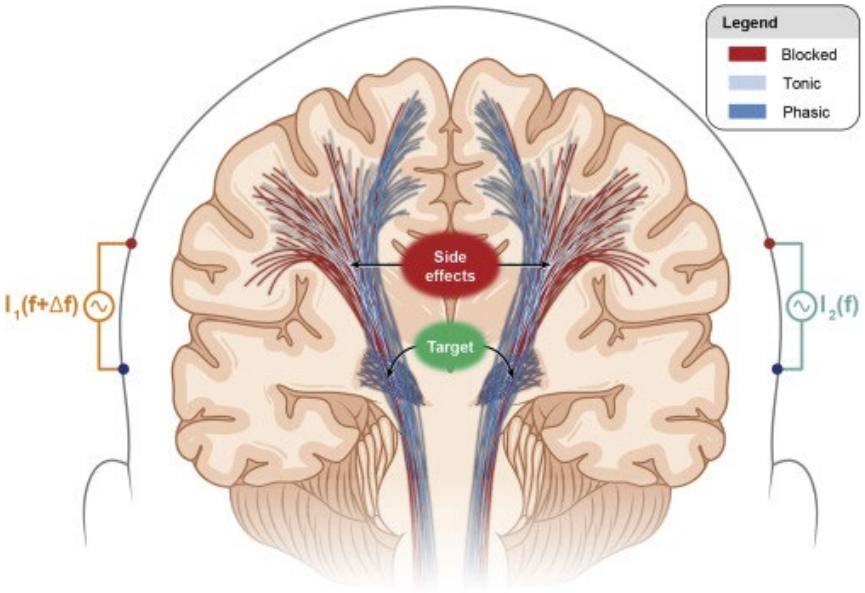

Mirzakhalili E et al., *Cell Systems*, 2020; 11, 557-572.e5

- Mirzakhalili 2020 [22]/ 2023 [45]: where TI drives firing (MRG/cortical models), spatial pattern is a "sandwich":
  - Near electrodes: carrier-driven activation/onset (suprathreshold direct kHz; pattern depends on compartment/regime).
  - Ring near target: modulated firing at Δf (envelope-following).
  - Volume between: kHz conduction block (sustained depolarization → Na^+ inactivation).
- Same active rectification produces both on-target envelope-following and off-target conduction.

- *Translation problem*: in human heads at 2 mA/ch, fields too weak for rectifying regime anywhere — neither envelope-following nor block. Mouse mechanism [21] does not easily scale.
- Macaque single-unit [46]: TI alters spike timing (envelope entrainment), not rate, consistent with sub-threshold biasing.

Candidate Mechanisms: Predictions & Limitations

Mechanism	Required field regime	Empirical status	Open concern
(1) Passive filtering	Any, if valid	Untenable: linear filter cannot create Δf from f_1, f_2 [22]	Original intuition [21], not operative
(2) Active rectification	Strong nonlinear fields; ~80 V/m at 2 kHz in slice [23]	Models [22, 45] + in vitro [23]	Human fields ≲0.5–1 V/m: far too weak
(3) Network entrainment	Subthreshold; state-dependent	Compatible with tACS-like entrainment [9, 33] and human frequency-specific effects [48]	Needs susceptible ongoing rhythm; selectivity unproven
(4) Spike-timing bias	Subthreshold	Macaque timing shift without rate change [46]	BOLD/behavior may miss or average timing effects

- Human evidence [27, 28, 48, 49] is most compatible with (3)/(4), but does not yet distinguish them. It argues against (1) and makes (2) unlikely at standard human doses.
- “Passive demodulation false” ≠ “TI false”.

Modeling Support: Human Head Studies

- Rampersad 2019 [47] — anisotropic FEM, exhaustive optimization (88 locations, 146M montages):
  - Mouse, 0.776 mA: peak envelope 383 V/m (suprathreshold, [21] consistent).
  - Human, ≤2 mA, 4 electrodes: peak envelope ≈ 0.57 V/m M1, 0.37 V/m pallidum, 0.24 V/m hippocampus.
  - Deep-target envelope ≈ tACS at depth, with less superficial exposure — modest modeling selectivity gain.
- Cadaver/intracranial measurements in [27] support hippocampal targeting and relative hippocampus-vs-cortex envelope contrast.
- Take-home: sub-threshold is the likely operating regime.

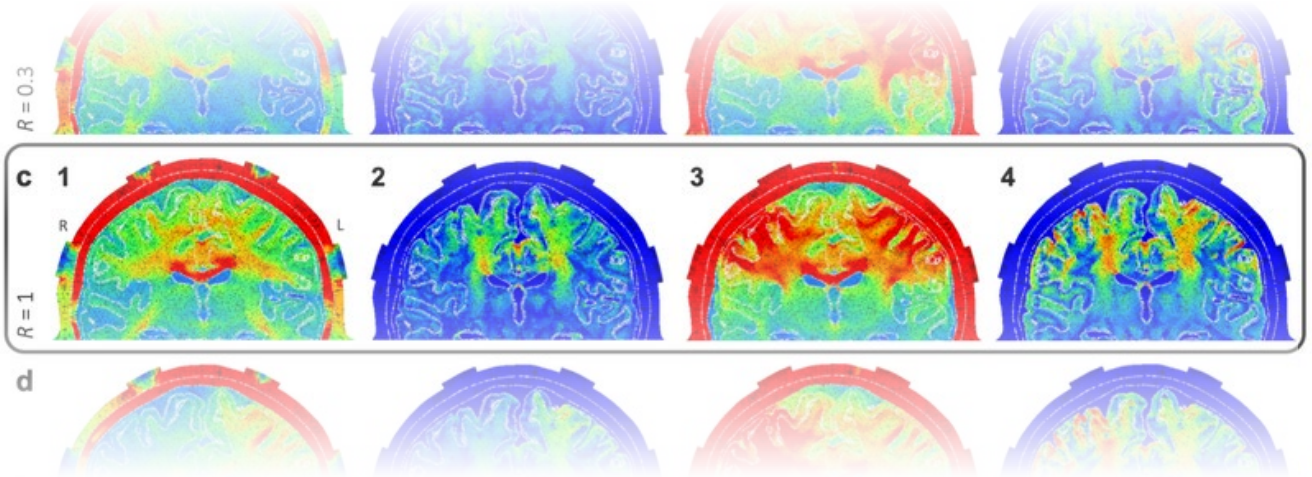

Field strengths on a coronal plane through the electrodes. From top to bottom, current ratio $R = I_R/I_L$ is increased from 0.1 to 10. c) R = 1.

Rampersad S, et al., *Neuroimage*. 2019 Nov 15;202:116124.

First human Deep-Target Evidence: Hippocampus

- Violante 2023 [27] — first focal non-invasive TI of a deep human structure.
  - Protocol: 2kHz carriers, Δf=5 Hz; in-vivo fMRI used TI 1:1 = 2 mA + 2 mA and TI 1:3 = 1 mA + 3 mA; concurrent fMRI during face–name memory task.
  - Modeling + cadaver: envelope peaks in HC (~0.26–0.40 V/m), > overlying cortex.
  - Online fMRI: focal hippocampal BOLD reduction; no cortical change; steered by current ratios.
  - Behavior: improved memory accuracy and confidence vs sham.
- Establishes: sub-threshold ~5 Hz envelope, focal to HC, produces measurable, behaviorally relevant modulation in humans.
- Does not establish a mechanism...

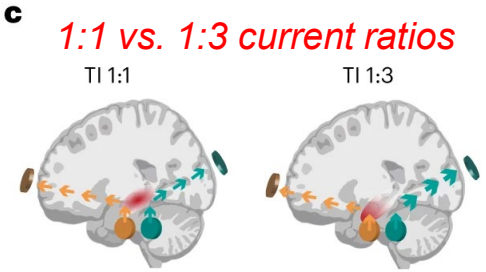

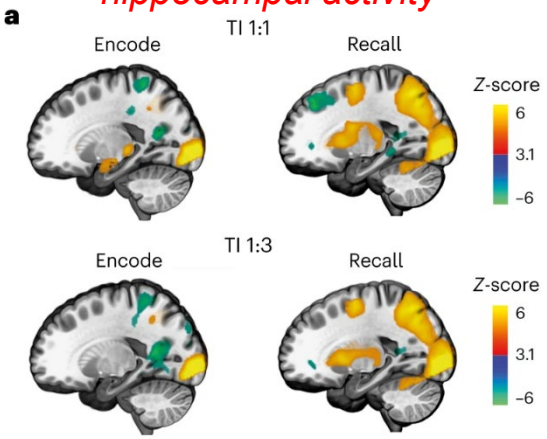

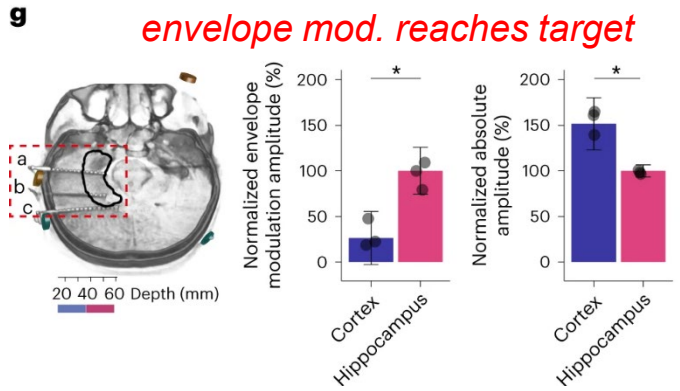

Violante, I.R. et al., *Nat Neurosci* **26**, 1994–2004 (2023).

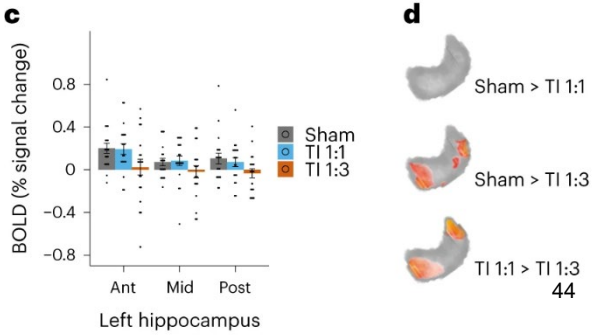

Intersubject Correlations: Region fMRI, Region Exposure, Behavior

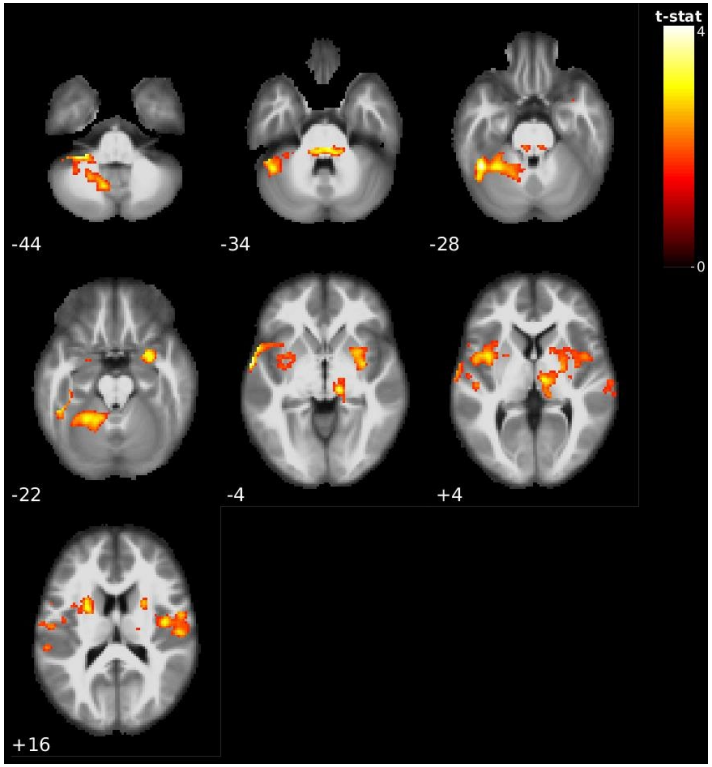

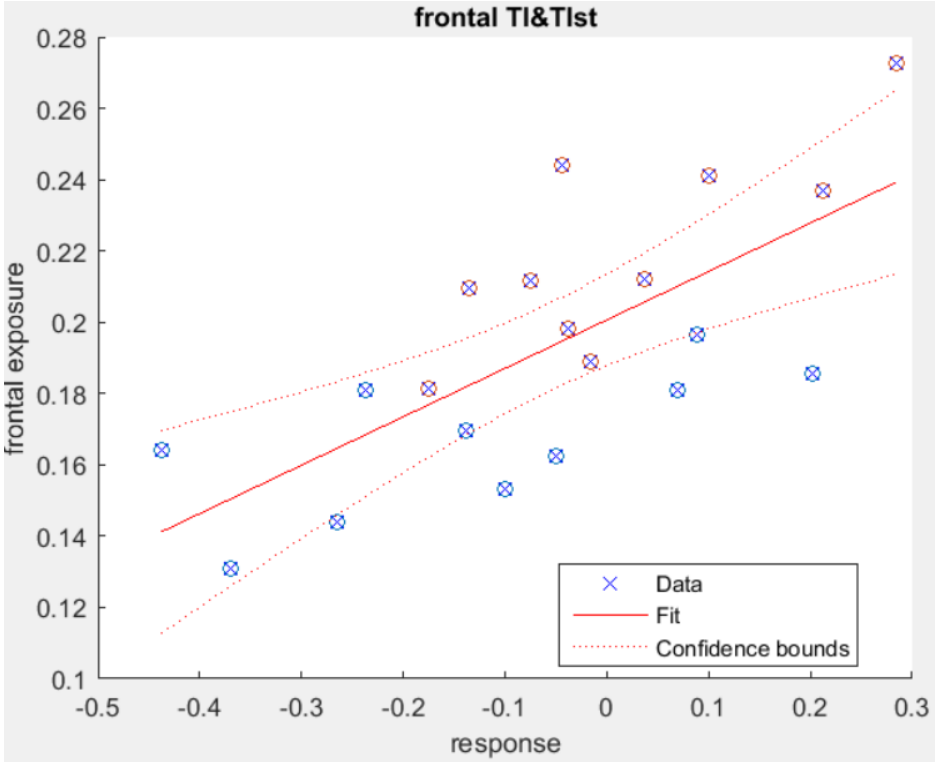

First Human Deep-Target Evidence: Hippocampus

Inter-subject variability is associated with differences in exposure…

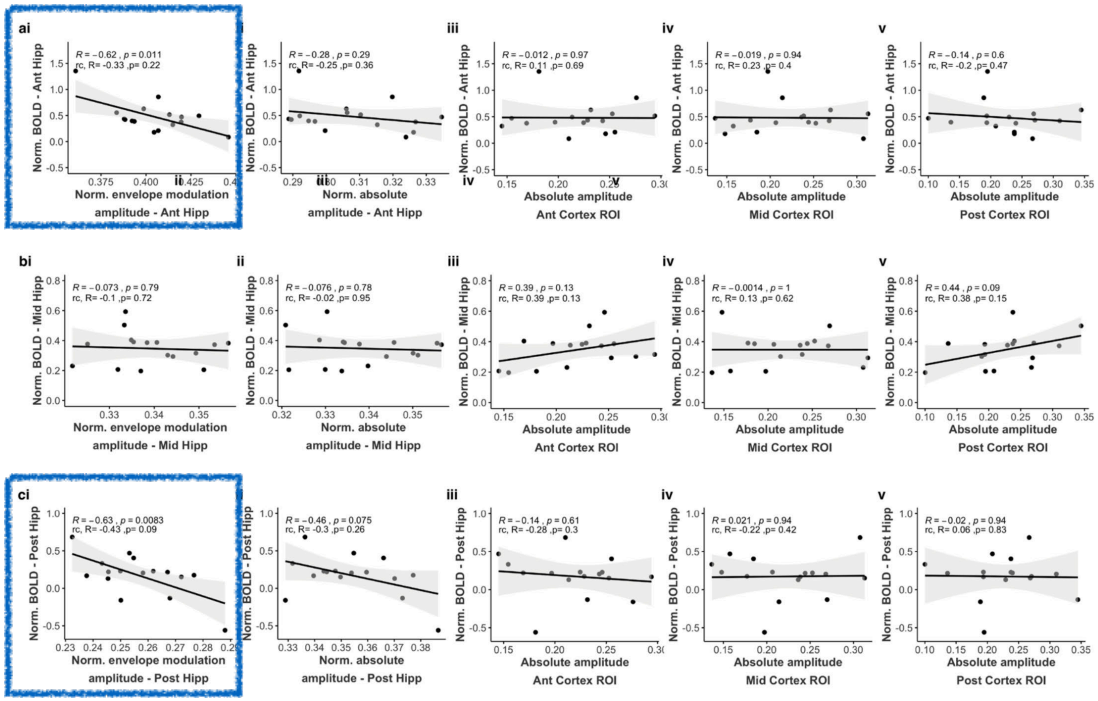

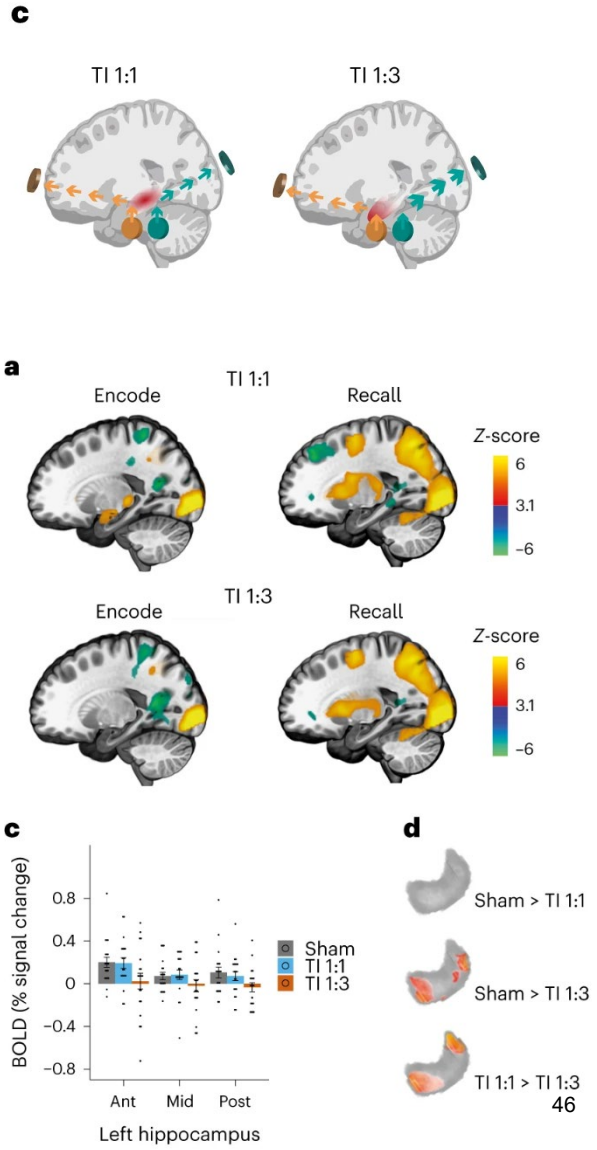

Violante, I.R. et al., *Nat Neurosci* **26**, 1994–2004 (2023).

Striatum, Hippocampal (HC)-Entorhinal Cortex (EC), and Motor Learning

- Striatal motor learning — Wessel/Beanato 2023 [28]: theta-burst tTIS (2 kHz, Δf=100 Hz iTBS); ↑ striatal BOLD + enhanced motor sequence learning, larger in older adults.
- Reinforcement learning (RL) — Vassiliadis/Beanato 2024 [48]: 2 kHz; Δf=80 Hz (gamma) disrupted RL gains; Δf=20 Hz (beta) did not. Frequency-specific causal effect.
- HC–EC navigation — Beanato 2024 [49]: tTIS to HC–EC during VR; reduced recall time; HC–EC-specific BOLD modulation.
- Negative results — von Conta 2022 [50]: tTIS vs tACS, parieto-occipital α (MEG, n=34): no tTIS aftereffect; failure of cortical-α entrainment. (n=34 moderate, *not decisive - very low currents used*); Zhang 2022 [54]: no diff. between TI and sham on working memory.
- Pattern: human evidence strongest when target is deep, readout task-dependent, envelope at a physiologically meaningful frequency for that target.

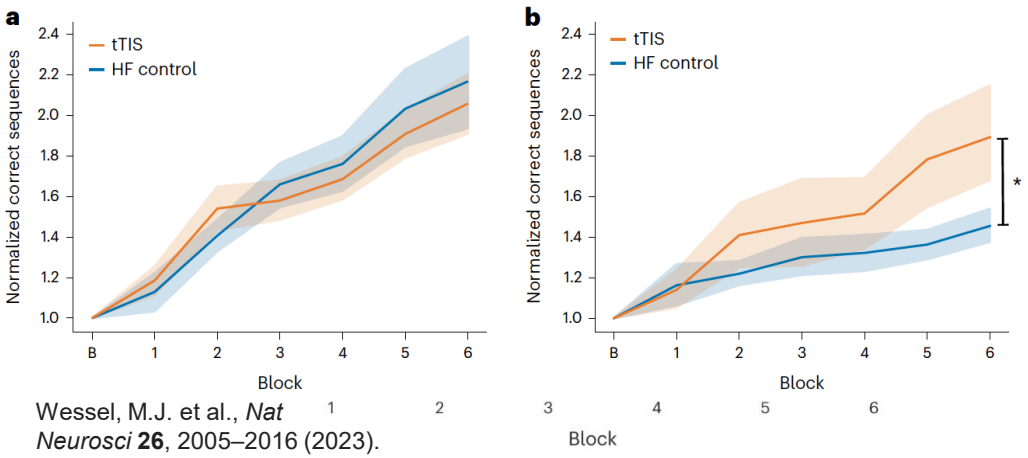

Wessel, M.J. et al., *Nat Neurosci* **26**, 2005–2016 (2023).

Left: correct key presses > in TIS vs. high-frequency (HF) control. ***Effect sizes increase when stratified by age.***

Right: areas in right striatum significantly modulated by correct key presses (HF had none)

Open Questions

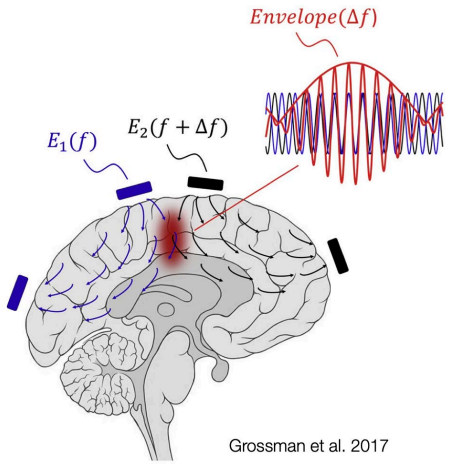

- **What we know**:
  - Envelope amplitudes (~0.2–0.5 V/m) and selectivity well-modeled, validated by cadaver/intracranial [27, 47].
  - Human studies: task-locked, anatomically specific BOLD + behavior at deep targets [27, 28, 48, 49].
  - Peripheral-nerve TI selectivity in rodents [30] — TI tested across anatomical contexts.
- **What is contested**:
  - Mechanism — passive demodulation unlikely [22]; active rectification needs suprathreshold [22, 45]; subthreshold possibly network/spike-time-dependent [23, 46].
  - Selectivity — unmodulated cortical kHz can exceed deep envelope [23]; in vivo importance unsettled; carrier frequency can be increased to compensate.
  - Cortical entrainment — one MEG study (n=34) finds no after-effect [50].
- **What is open**:
  - Optimal f_c (no consensus optimum; convention 2 kHz [21, 27, 28]; recent 9/20 kHz [43, 44]; higher carriers up to 80 kHz also reported)
  - Whether TIS imposes new oscillations or biases ongoing ones [46].
  - How envelope effects scale across populations, states, pathology.

Outline for Today

- Modalities at a glance — tDCS, tACS, TMS
- Modeling tES forward fields — quasi-static, lead fields, somatic-polarization rule
- TMS field modeling and clinical translation — coil topographies, dosing, indications
- Temporal interference — the idea, the biophysics debate, recent human evidence
- **Treatment planning & optimization — multi-objective targeting**
- Exercise preview: Reto Huber (KISPI) — Non-invasive electric & acoustic brain stimulation

TIP: The IT'IS TI Planning Tool

- TIP — IT'IS TI planning workflow [10].
- Pipeline [10]:
  - Inputs: T1 (DWI), target ROI, 10–10 search space, optimization weights.
  - Segmentation: 3D U-Net (head16/30/40); <5 min vs ~30 min CHARM, ~1 h headreco.
  - EM solver: Sim4Life EQS, voxel mesh; one solve per electrode → E-field basis.
  - Optimization: exhaustive grid search via basis superposition; Pareto front for (M1, M2, M3: *see next slide*).
  - Outputs: key metrics (M1, M2, M3), positions, per-channel currents, envelope maps, Pareto front, interactive exposure analysis.
- Backends: (i) precomputed bases on reference human and animal models (fast, generic); (ii) end-to-end personalized from MRI (slower).
- Optimization: Gaussian process modeling with a multi-objective genetic algorithm—explores the solution space to provide a diverse set of Pareto-optimal solutions (W11).
- Alternatives: SimNIBS [16, 38] and ROAST [53] solve the tES forward problem but lack native TI-specific multi-objective Pareto optimization.

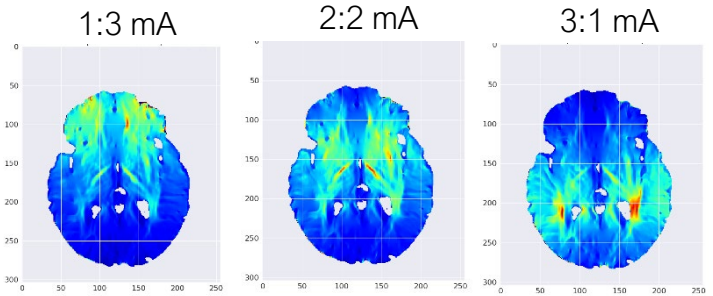

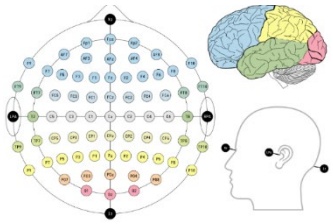

Electrode Setup

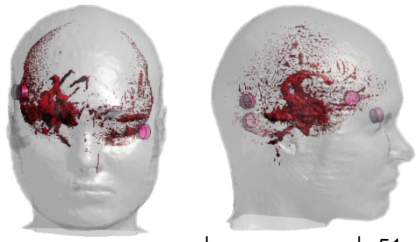

Multi-Objective Optimization

- Three objectives [10]:
  - M1 — Strength: maximize median (or p-th percentile) envelope in target ROI.
  - M2 — Selectivity: maximize ratio of mean envelope target/off-target.
  - M3 — Collateral: minimize off-target volume fraction where envelope exceeds M1.
- No single optimum — these conflict. Deliverable is a Pareto front, not a point; user selects an operating point on the front.
- Pareto framing generalizes — TMS coil placement, tDCS HD montages, DBS contact selection (W07).

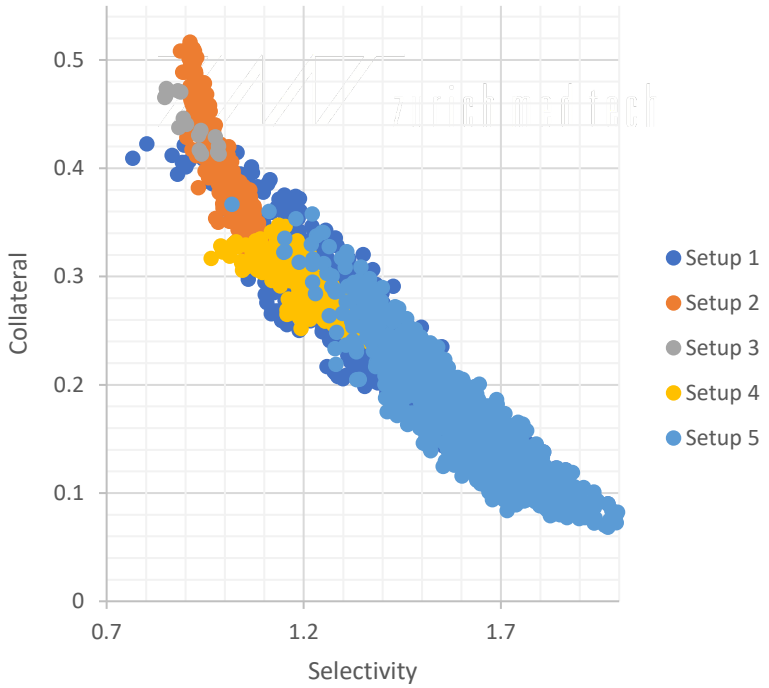

TIS vs. tACS: head-to-head

Metric	tACS (2 mA peak-to-peak)	TIS (deep target, 2x1 mA, 4-electrode optimized)
(a) Target drive	Cortical peak E-field ~0.3–0.5 V/m for typical 2 mA p-p tACS; montage-dependent [56, 57]	Example: ~0.24 V/m *envelope modulation* in hippocampus (HC), ~0.37 V/m in pallidum [47, 27]
(b) Superficial unmodulated	N/a— no kHz carrier; off-target field is at the stimulation frequency.	Cortical kHz can ≥ deep envelope (e.g., 0.48 vs 0.36 V/m per mA [23])
(c) Total current	2 mA peak-to-peak (= ±1 mA peak)	2 mA (two channels at 1 mA each)
(d) Target/cortex contrast	Poor deep/cortex contrast; montage diffuse	Can improve deep-target selectivity, but magnitude and focality are target-, metric-, and montage-dependent [47].

TIS favored when:

- Target is deep (HC, striatum, pallidum), enough distance from cortex for envelope contrast [27, 28, 47].
- Readout state- or frequency-specific (entrainment, theta-burst); envelope can be patterned [28].
- Personalization feasible (T1 MRI; W11) [10].
- Simultaneous EEG and fMRI recording feasible -> phase synchronization and closed-loop possible

TIS does not beat tDCS/tACS when:

- Target is cortical — TIS sacrifices envelope for selectivity the others don't need; superficial kHz becomes a liability [23, 50].

Summary & Key Takeaways

- Same modeling approach as for sensing, but opposite direction. W09 lead-field framework, arrow reversed; reciprocity does the algebra (bilinear, not matrix transpose).
- tES is sub-threshold. ~0.3 V/m × 0.2 mV/(V/m) → tens of μV bias; effects accumulate by biasing networks near threshold [1][3]–[7].
- TMS = the other Maxwell route. Faraday-induced E ($\partial B/\partial t$), suprathreshold, selective for axonal microgeometry (bends/terminations/σ-contrast) via the activating function [11, 12, 52]. Clinical: MDD, OCD, addiction [24, 26, 39, 40]; cautionary in stroke [41].
- TIS: deep, focal envelope. Quantities-of-interest correlate with amplitude modulation; demodulation is contested [21, 22, 23, 46]. Of four mechanisms, human evidence compatible with network entrainment + spike-timing bias [27, 28, 48, 49].
- Optimization is multi-objective. Strength, selectivity, collateral conflict; deliverable is a Pareto front, not a point. TIP [10] operationalizes for TI; machinery → W11.
- Personalization is highly encouraged: Inter-subject E-field variability is large [29]; generic montages → generic outcomes.

Exercise: Guest Lecture (Prof. Reto Huber)

Mini project reminder

- Apply concepts from Weeks 1–8 to your chosen project topic
- Consider the abstraction-level question for your own project:
  - What is the minimum level of biophysical detail your question requires?
  - Where can you simplify without changing the answer?
- Office hours available for project consultation
- Project presentations in Week 13 (28.05.2026)

Upcoming guest lecture schedule:

- **Today**: Prof. Reto Huber (Zurich Children's Hospital)—Non-Invasive *Electric and Acoustic Brain Stimulation*
- **May 7th**: Prof. Henri Lorach (UNIL)—*Spinal Cord Stimulation*

References

[1] T. Radman, R. L. Ramos, J. C. Brumberg, M. Bikson. "Role of cortical cell type and morphology in subthreshold and suprathreshold uniform electric field stimulation in vitro." Brain Stimul. 2(4):215–228, 2009. doi:10.1016/j.brs.2009.03.007.
[2] M. Bikson, M. Inoue, H. Akiyama, J. K. Deans, J. E. Fox, H. Miyakawa, J. G. R. Jefferys. "Effects of uniform extracellular DC electric fields on excitability in rat hippocampal slices in vitro." J. Physiol. 557(Pt 1):175–190, 2004. doi:10.1113/jphysiol.2003.055772.
[3] A. Datta, V. Bansal, J. Diaz, J. Patel, D. Reato, M. Bikson. "Gyri-precise head model of transcranial direct current stimulation: improved spatial focality using a ring electrode versus conventional rectangular pad." Brain Stimul. 2(4):201–207.e1, 2009. doi:10.1016/j.brs.2009.03.005.
[4] R. J. Sadleir, T. D. Vannorsdall, D. J. Schretlen, B. Gordon. "Transcranial direct current stimulation (tDCS) in a realistic head model." NeuroImage 51(4):1310–1318, 2010. doi:10.1016/j.neuroimage.2010.03.052.
[5] A. Opitz et al. "Spatiotemporal structure of intracranial electric fields induced by transcranial electric stimulation in humans and nonhuman primates." Sci. Rep. 6:31236, 2016. doi:10.1038/srep31236.
[6] Y. Huang et al. "Measurements and models of electric fields in the in vivo human brain during transcranial electric stimulation." eLife 6:e18834, 2017. doi:10.7554/eLife.18834. Corrigendum: eLife 7:e35178, 2018. doi:10.7554/eLife.35178.
[7] M. A. Nitsche, W. Paulus. "Excitability changes induced in the human motor cortex by weak transcranial direct current stimulation." J. Physiol. 527(Pt 3):633–639, 2000. doi:10.1111/j.1469-7793.2000.t01-1-00633.x.
[8] A. Antal, K. Boros, C. Poreisz, L. Chaieb, D. Terney, W. Paulus. "Comparatively weak after-effects of transcranial alternating current stimulation (tACS) on cortical excitability in humans." Brain Stimul. 1(2):97–105, 2008. doi:10.1016/j.brs.2007.10.001.
[9] R. F. Helfrich, T. R. Schneider, S. Rach, S. A. Trautmann-Lengsfeld, A. K. Engel, C. S. Herrmann. "Entrainment of brain oscillations by transcranial alternating current stimulation." Curr. Biol. 24(3):333–339, 2014. doi:10.1016/j.cub.2013.12.041.
[10] F. Karimi, M. Steiner, T. Newton, B. A. A. Lloyd, A. M. Cassarà, P. de Fontenay, S. Farcito, J. P. Triebkorn, E. Beanato, H. , E. Iavarone, F. C. Hummel, N. Kuster, V. Jirsa, E. Neufeld. "Precision non-invasive brain stimulation: an in silico pipeline for personalized control of brain dynamics." J. Neural Eng. 22(2):026061, 2025. doi:10.1088/1741-2552/adb88f.
[11] B. J. Roth, P. J. Basser. "A model of the stimulation of a nerve fiber by electromagnetic induction." IEEE Trans. Biomed. Eng. 37(6):588–597, 1990. doi:10.1109/10.55662.
[12] P. J. Maccabee, V. E. Amassian, L. P. Eberle, R. Q. Cracco. "Magnetic coil stimulation of straight and bent amphibian and mammalian peripheral nerve in vitro: locus of excitation." J. Physiol. 460:201–219, 1993. doi:10.1113/jphysiol.1993.sp019467.
[13] P. M. Rossini et al. "Non-invasive electrical and magnetic stimulation of the brain, spinal cord and roots: basic principles and procedures for routine clinical application. Report of an IFCN committee." Electroencephalogr. Clin. Neurophysiol. 91(2):79–92, 1994. doi:10.1016/0013-4694(94)90029-9.
[14] S. Rossi et al. "Safety and recommendations for TMS use in healthy subjects and patient populations, with updates on training, ethical and regulatory issues: Expert guidelines." Clin. Neurophysiol. 132(1):269–306, 2021. doi:10.1016/j.clinph.2020.10.003.
[15] S. Rossi, M. Hallett, P. M. Rossini, A. Pascual-Leone (Safety of TMS Consensus Group). "Safety, ethical considerations, and application guidelines for the use of transcranial magnetic stimulation in clinical practice and research." Clin. Neurophysiol. 120(12):2008–2039, 2009. doi:10.1016/j.clinph.2009.08.016.
[16] A. Thielscher, A. Antunes, G. B. Saturnino. "Field modeling for transcranial magnetic stimulation: a useful tool to understand the physiological effects of TMS?" EMBC 2015:222–225. doi:10.1109/EMBC.2015.7318340.
[17] S. Ueno, T. Tashiro, K. Harada. "Localized stimulation of neural tissues in the brain by means of a paired configuration of time-varying magnetic fields." J. Appl. Phys. 64(10):5862–5864, 1988. doi:10.1063/1.342181.
[18] Y. Roth, A. Zangen, M. Hallett. "A coil design for transcranial magnetic stimulation of deep brain regions." J. Clin. Neurophysiol. 19(4):361–370, 2002. doi:10.1097/00004691-200208000-00008.
[19] A. Zangen, Y. Roth, B. Voller, M. Hallett. "Transcranial magnetic stimulation of deep brain regions: evidence for efficacy of the H-coil." Clin. Neurophysiol. 116(4):775–779, 2005. doi:10.1016/j.clinph.2004.11.008.
[20] E. R. Lontis, M. Voigt, J. J. Struijk. "Focality assessment in transcranial magnetic stimulation with double and cone coils." J. Clin. Neurophysiol. 23(5):462–471, 2006. doi:10.1097/01.wnp.0000229944.63011.a1.

References

[21] N. Grossman et al. "Noninvasive Deep Brain Stimulation via Temporally Interfering Electric Fields." Cell 169(6):1029–1041.e16, 2017. doi:10.1016/j.cell.2017.05.024.
[22] E. Mirzakhalili, B. Barra, M. Capogrosso, S. F. Lempka. "Biophysics of Temporal Interference Stimulation." Cell Syst. 11(6):557–572.e5, 2020. doi:10.1016/j.cels.2020.10.004.
[23] Z. Esmaeilpour, G. Kronberg, D. Reato, L. C. Parra, M. Bikson. "Temporal interference stimulation targets deep brain regions by modulating neural oscillations." Brain Stimul. 14(1):55–65, 2021. doi:10.1016/j.brs.2020.11.007.
[24] J. P. O'Reardon et al. "Efficacy and safety of transcranial magnetic stimulation in the acute treatment of major depression: a multisite randomized controlled trial." Biol. Psychiatry 62(11):1208–1216, 2007. doi:10.1016/j.biopsych.2007.01.018.
[25] L. L. Carpenter et al. "Transcranial magnetic stimulation (TMS) for major depression: a multisite, naturalistic, observational study of acute treatment outcomes in clinical practice." Depress. Anxiety 29(7):587–596, 2012. doi:10.1002/da.21969.
[26] E. J. Cole et al. "Stanford Accelerated Intelligent Neuromodulation Therapy for Treatment-Resistant Depression." Am. J. Psychiatry 177(8):716–726, 2020. doi:10.1176/appi.ajp.2019.19070720. [26b] E. J. Cole et al. "Stanford Neuromodulation Therapy (SNT): A double-blind randomized controlled trial." Am. J. Psychiatry 179(2):132–141, 2022. doi:10.1176/appi.ajp.2021.20101429.
[27] I. R. Violante et al. "Non-invasive temporal interference electrical stimulation of the human hippocampus." Nat. Neurosci. 26(11):1994–2004, 2023. doi:10.1038/s41593-023-01456-8.
[28] M. J. Wessel*, E. Beanato* et al. "Noninvasive theta-burst stimulation of the human striatum enhances striatal activity and motor skill learning." Nat. Neurosci. 26(11):2005–2016, 2023. doi:10.1038/s41593-023-01457-7.
[29] J. von Conta, F. H. Kasten, B. Ćurčić-Blake, A. Aleman, A. Thielscher, C. S. Herrmann. "Interindividual variability of electric fields during transcranial temporal interference stimulation (tTIS)." Sci. Rep. 11:20357, 2021. doi:10.1038/s41598-021-99749-0.
[30] B. Botzanowski et al. "Noninvasive Stimulation of Peripheral Nerves using Temporally-Interfering Electrical Fields." Adv. Healthc. Mater. 11(17):2200075, 2022. doi:10.1002/adhm.202200075.
[31] A. M. Cassarà, T. H. Newton, K. Zhuang, S. J. Regel, P. Achermann, A. Pascual-Leone, N. Kuster, E. Neufeld. "Recommendations for the Safe Application of Temporal Interference Stimulation in the Human Brain Part II: Biophysics, Dosimetry, and Safety Recommendations." Bioelectromagnetics 46(1):e22536, 2025. doi:10.1002/bem.22536.
[32] A. M. Cassarà, T. H. Newton, K. Zhuang, S. J. Regel, P. Achermann, A. Pascual-Leone, N. Kuster, E. Neufeld. "Recommendations for the Safe Application of Temporal Interference Stimulation in the Human Brain Part I: Principles of Electrical Neuromodulation and Adverse Effects." Bioelectromagnetics 46(2):e22542, 2025. doi:10.1002/bem.22542.
[33] W. A. Huang et al. "Transcranial alternating current stimulation entrains alpha oscillations by preferential phase synchronization of fast-spiking cortical neurons to stimulation waveform." Nat. Commun. 12:3151, 2021. doi:10.1038/s41467-021-23021-2.
[34] R. Kanai, L. Chaieb, A. Antal, V. Walsh, W. Paulus. "Frequency-dependent electrical stimulation of the visual cortex." Curr. Biol. 18(23):1839–1843, 2008. doi:10.1016/j.cub.2008.10.027.
[35] P. A. Hasgall, F. Di Gennaro, C. Baumgartner, E. Neufeld, B. Lloyd, M. C. Gosselin, D. Payne, A. Klingenböck, N. Kuster. IT'IS Database for Thermal and Electromagnetic Parameters of Biological Tissues, v4.1, 2022. doi:10.13099/VIP21000-04-1.
[36] M. Bikson, J. P. Dmochowski, A. Rahman. "The 'quasi-uniform' assumption in animal and computational models of non-invasive electrical stimulation." Brain Stimul. 6(4):704–705, 2013. doi:10.1016/j.brs.2013.03.001.
[37] Z.-D. Deng, S. H. Lisanby, A. V. Peterchev. "Electric field depth–focality tradeoff in transcranial magnetic stimulation: simulation comparison of 50 coil designs." Brain Stimul. 6(1):1–13, 2013. doi:10.1016/j.brs.2012.02.005.
[38] G. B. Saturnino, K. H. Madsen, A. Thielscher. "Electric field simulations for transcranial brain stimulation using FEM: an efficient implementation and error analysis." J. Neural Eng. 16(6):066032, 2019. doi:10.1088/1741-2552/ab41ba.
[39] L. Carmi et al. "Efficacy and safety of deep transcranial magnetic stimulation for obsessive-compulsive disorder: a prospective multicenter randomized double-blind placebo-controlled trial." Am. J. Psychiatry 176(11):931–938, 2019. doi:10.1176/appi.ajp.2019.18101180.
[40] A. Zangen et al. "Repetitive transcranial magnetic stimulation for smoking cessation: a pivotal multicenter double-blind randomized controlled trial." World Psychiatry 20(3):397–404, 2021. doi:10.1002/wps.20905.

References

[41] R. L. Harvey et al. (NICHE Trial Investigators). "Randomized sham-controlled trial of navigated repetitive transcranial magnetic stimulation for motor recovery in stroke (NICHE)." Stroke 49(9):2138–2146, 2018. doi:10.1161/STROKEAHA.117.020607.
[42] B. Hutcheon, Y. Yarom. "Resonance, oscillation and the intrinsic frequency preferences of neurons." Trends Neurosci. 23(5):216–222, 2000. doi:10.1016/S0166-2236(00)01547-2.
[43] Y. , G. Q. Zeng, M. , M. Zhang, C. Chang, Q. Liu, K. , R. Ma, Y. , X. Zhang. "The safety and efficacy of applying a high-current temporal interference electrical stimulation in humans." Front. Hum. Neurosci. 18:1484593, 2024. doi:10.3389/fnhum.2024.1484593.
[44] F. Missey, E. Acerbo, A. S. Dickey et al. "Non-invasive temporal interference stimulation of the hippocampus suppresses epileptic biomarkers in patients with epilepsy: biophysical differences between kilohertz and amplitude modulated stimulation." Brain Stimul. 19(1):102981, 2025/2026. doi:10.1016/j.brs.2025.11.008.
[45] B. , A. S. Aberra, W. M. Grill, A. V. Peterchev. "Responses of model cortical neurons to temporal interference stimulation and related transcranial alternating current stimulation modalities." J. Neural Eng. 19(6):066047, 2023. doi:10.1088/1741-2552/acab30.
[46] P. G. Vieira, M. R. Krause, C. C. Pack. "Temporal interference stimulation disrupts spike timing in the primate brain." Nat. Commun. 15:4558, 2024. doi:10.1038/s41467-024-48962-2.
[47] S. Rampersad et al. "Prospects for transcranial temporal interference stimulation in humans: A computational study." NeuroImage 202:116124, 2019. doi:10.1016/j.neuroimage.2019.116124.
[48] P. Vassiliadis, E. Beanato et al. "Non-invasive stimulation of the human striatum disrupts reinforcement learning of motor skills." Nat. Hum. Behav. 8(8):1581–1598, 2024. doi:10.1038/s41562-024-01901-z.
[49] E. Beanato et al. "Noninvasive modulation of the hippocampal-entorhinal complex during spatial navigation in humans." Sci. Adv. 10(44):eado4103, 2024. doi:10.1126/sciadv.ado4103.
[50] J. von Conta, F. H. Kasten, K. Schellhorn, B. Ćurčić-Blake, A. Aleman, C. S. Herrmann. "Benchmarking the effects of transcranial temporal interference stimulation (tTIS) in humans." Cortex 154:299–310, 2022. doi:10.1016/j.cortex.2022.05.017.
[51] H. McCann, G. Pisano, L. Beltrachini. "Variation in reported human head tissue electrical conductivity values." Brain Topogr. 32(5):825–858, 2019. doi:10.1007/s10548-019-00710-2.
[52] F. Rattay. "Analysis of models for external stimulation of axons." IEEE Trans. Biomed. Eng. 33(10):974–977, 1986. doi:10.1109/TBME.1986.325670.
[53] Y. Huang, A. Datta, M. Bikson, L. C. Parra. "Realistic volumetric-approach to simulate transcranial electric stimulation — ROAST — a fully automated open-source pipeline." J. Neural Eng. 16(5):056006, 2019. doi:10.1088/1741-2552/ab208d.
[54] Zhang Y, Zhou Z, Zhou J, Qian Z, Lü J, Li L and Liu Y (2022) Temporal interference stimulation targeting right frontoparietal areas enhances working memory in healthy individuals. Front. Hum. Neurosci. 16:918470. doi: 10.3389/fnhum.2022.918470
[55] Acerbo E, Jegou A, Luff C, Dzialecka P, Botzanowski B, Missey F, Ngom I, Lagarde S, Bartolomei F, Cassara A, Neufeld E, Jirsa V, Carron R, Grossman N and Williamson A (2022) Focal non-invasive deep-brain stimulation with temporal interference for the suppression of epileptic biomarkers. Front. Neurosci. 16:945221. doi: 10.3389/fnins.2022.945221
[56] Huang Y, Datta A, Bikson M, Parra LC. Realistic volumetric-approach to simulate transcranial electric stimulation-ROAST-a fully automated open-source pipeline. J Neural Eng. 2019 Jul 30;16(5):056006. doi: 10.1088/1741-2552/ab208d. PMID: 31071686; PMCID: PMC7328433.
[57] Opitz, A., Falchier, A., Yan, CG. et al. Spatiotemporal structure of intracranial electric fields induced by transcranial electric stimulation in humans and nonhuman primates. Sci Rep 6, 31236 (2016). https://doi.org/10.1038/srep31236
[58] International Commission on Non-Ionizing Radiation Protection, "ICNIRP guidelines for limiting exposure to time-varying electric and magnetic fields (1 Hz – 100 kHz)," *Health Phys.*, vol. 99, no. 6, pp. 818–836, 2010, doi: 10.1097/HP.0b013e3181f06c86.